DISSERTATIONES
CHIMICAE
UNIVERSITATIS
TARTUENSIS
162

TAAVI IVAN

Bifunctional inhibitors and photoluminescent probes for studies on protein complexes

DISSERTATIONES CHIMICAE UNIVERSITATIS TARTUENSIS
162

DISSERTATIONES CHIMICAE UNIVERSITATIS TARTUENSIS
162

TAAVI IVAN

Bifunctional inhibitors and photoluminescent probes for studies on protein complexes

UNIVERSITY OF TARTU
Press

Institute of Chemistry, Faculty of Science and Technology, University of Tartu, Estonia

Dissertation was accepted for the commencement of the degree of *Doctor philosophiae* in Chemistry at the University of Tartu on June 14th, 2017 by the Council of Institute of Chemistry, Faculty of Science and Technology, University of Tartu.

Supervisors: Asko Uri, PhD
Institute of Chemistry, University of Tartu, Estonia
Kaido Viht, PhD
Institute of Chemistry, University of Tartu, Estonia

Opponent: Dr. Matthias Joseph Knape, University of Kassel, Germany

Commencement: August 21, 2017 at 12:00, room 1021, 14A Ravila St., Institute of Chemistry, University of Tartu

This research was supported by grants from the Estonian Research Council (IUT20-17), the Estonian Science Foundation (8230, 8419, and 8055), from the Estonian Ministry of Education and Sciences (SF0180121s08), from British Heart Foundation (PG/10/75/28537 and RG/12/3/29423), from Norwegian Research Council (Project 183376), and from the Graduate School "Functional materials and technologies", receiving funding from the European Regional Development Fund; by the national scholarship program Kristjan Jaak, which is funded by Archimedes Foundation.

ISSN 1406-0299
ISBN 978-9949-77-499-9 (print)
ISBN 978-9949-77-500-2 (pdf)

Copyright: Taavi Ivan, 2017

University of Tartu Press
www.tyk.ee

CONTENTS

LIST OF ORIGINAL PUBLICATIONS

I E. Enkvist, A. Vaasa, M. Kasari, M. Kriisa, **T. Ivan**, K. Ligi, G. Raidaru, A. Uri, Protein-induced long lifetime luminescence of nonmetal probes, ACS Chem. Biol. 6 (2011) 1052–1062.

II **T. Ivan**, E. Enkvist, B. Viira, G.B. Manoharan, G. Raidaru, A. Pflug, K.A. Alam, M. Zaccolo, R.A. Engh, A. Uri, Bifunctional ligands for inhibition of tight-binding protein-protein interactions, Bioconjug. Chem. 27 (2016) 1900–1910.

III H. Sinijarv, S. Wu, **T. Ivan**, T. Laasfeld, K. Viht, A. Uri, Binding assay for characterization of protein kinase inhibitors possessing sub-picomolar to sub-millimolar affinity, Anal. Biochem. 531 (2017) 67–77.

IV **T. Ivan**, E. Enkvist, H. Sinijarv, A. Uri, Competitive ligands facilitate dissociation of the complex of bifunctional inhibitor and protein kinase, Biophys. Chem. 228 (2017) 17–24.

Author's contribution:

Paper I: The author participated in designing of experiments, introduced the setup of kinetic measurements, carried out the proportion of experiments with ARC-Lum(Fluo) probes and analysis of respective results.

Paper II: The author purified and characterized the set of 4-(piperazin-1-yl)-7H-pyrrolo[2,3-d]pyrimidine compounds, was responsible for the design of most experiments, performed thermal shift assay and lysate experiments, conducted data analysis, and wrote the bulk of the manuscript.

Paper III: The author provided technical advice, produced PKAc, and participated in data analysis and writing of the manuscript.

Paper IV: The author designed and performed experiments and was responsible for data analysis and writing of the manuscript.

ABBREVIATIONS

AA	amino acid
AC	adenylate cyclase
Adc	adenosine 4'-dehydroxymethyl-4'-carboxylic acid moiety
Ahx	6-aminohexanoic acid moiety
AMSE	5-(2-aminopyrimidin-4-yl)selenophene-2-carboxylic acid moiety
AMTH	5-(2-aminopyrimidin-4-yl)thiophene-2-carboxylic acid moiety
ARC	adenosine analogue and oligoarginine conjugate
ARC-902	Adc-Ahx-(*D*Arg)$_6$-NH$_2$
ARC-1063	AMTH-Ahx-*D*Arg-Ahx-(*D*Arg)$_6$-*D*Lys(Alexa Fluor 647)-NH$_2$
ARC-1139	AMSE-Ahx-*D*Arg-Ahx-(*D*Arg)$_6$-*D*Lys(PromoFluor-647)-NH$_2$
ARC-1182	Adc-Ahx-*D*Arg-Ahx-(*D*Arg)$_6$-*D*Lys(PromoFluor-647)-NH$_2$
ARC-Lum	ARC-type probe possessing protein-induced luminescence signal with microsecond-scale lifetime
ARC-Lum(Fluo)	ARC-Lum probe conjugated with a fluorescent dye
ATP	adenosine-5'-triphosphate
C9H6	Chinese hamster ovary cell line stably expressing genetically engineered PKA subunits
cAMP	cyclic adenosine 3',5'-monophosphate
FA	fluorescence anisotropy
FRET	Förster-type resonant energy transfer
H89	N-[2-bromocinnamylamino)ethyl]-5-isoquinoline sulfonamide
His-tag	AA sequence of hexahistidine
HTS	high-throughput screening
IC_{50}	half maximal inhibitory concentration
ITC	isothermal titration calorimetry
K_D	equilibrium dissociation constant determined by direct binding
K_d	equilibrium displacement constant
k_{off}	dissociation rate constant for full break up of complex
$k_{d,n}/k_{a,n}$	individual dissociation/association rate constant
k_{on}	total association rate constant
PEG	polyethylene glycol
PKA	cAMP-dependent protein kinase A holoenzyme
PKAc	catalytic subunit of PKA
PKAr	regulatory subunit of PKA
PKB(Akt)	protein kinase B, RAC Ser/Thr protein kinase, gene name AKT

PKI	natural heat-stable peptide inhibitor of PKAc
PPI	protein-protein interaction
ROCK	Rho-associated protein kinase
SAR	structure-affinity relationship
SPR	surface plasmon resonance
TR	time-resolved
TR-FRET	time-resolved Förster-type resonant energy transfer
TRL	time-resolved luminescence

1. INTRODUCTION

A living cell is a highly complex and dynamic system. Proteins have the leading role in cellular signaling by participating in non-covalent interactions and catalyzing enzymatic reactions. Key regulators of signaling pathways are protein kinases (Bononi *et al.* 2011). Intracellular information exchange (signal transduction) between chromosome and extracellular matrix through a single pathway alone involves a cascade of protein kinases. While each step within signal mediation is conserved, significant cross-talk between different pathways can occur (Nishi *et al.* 2015). Abnormal activity of protein kinases, frequently resulting from altered gene expression (Schenk and Snaar-Jagalska 1999), entail many diseases that are difficult to address in terms of therapy (Yoeli-Lerner *et al.* 2006). In normally functioning signal transduction, a specific interaction between at least two proteins is necessary. Interactions between protein complexes that do not involve enzymatic reaction can be defined by the strength of interaction. Such protein-protein interactions (PPIs) range from very weak to very strong, depending on the contact area of interacting proteins and amino acid "hot spots" involved (Chen *et al.* 2013). There is increasing evidence of health disorders resulting from the defects in the formation of protein complexes. This knowledge has led the construction of compounds that disrupt or reinforce the interaction between proteins for therapeutic uses (Arkin *et al.* 2014; Wells and McClendon 2007; Thiel *et al.* 2012).

Various methods have been developed for studying the diverse superfamily of protein kinases, PPIs, and related small molecule ligands (Rao *et al.* 2014; Glickman 2012). Among these, fluorescence anisotropy (FA)- and Förster-type resonant energy transfer (FRET)-based methods are widely used due to their relative simplicity.

In this thesis, novel protein binding-responsive organic bifunctional probes (ARC-Lum probes) possessing long-lifetime (microsecond scale) photoluminescence were characterized in protein kinase binding assays in time-resolved (TR) format. This setup greatly reduced some of the shortcomings of FA- or fluorescence intensity (FI)-based assays, such as background fluorescence, leading to superior outcome in biochemical assays, and demonstrated the capability to monitor the activity of protein kinases in cells. The low TR signal of unbound ARC-Lum probes revealed their potential in the characterization of dissociation kinetics of a complex between protein kinase and competitive inhibitor. Kinetic characterization of biocomplexes may reveal crucial mechanistic information, not available from equilibrium constants. Measurement of rate constants in various applications led to the finding that bifunctional ligands behave differently from monofunctional ligands – the dissociation of a complex between a bifunctional ligand and target protein is facilitated by competitive inhibitors.

The application of ARC-Lum probes together with the TR measurement mode allowed the characterization of a new series of bifunctional ligands

possessing affinities down to one-digit picomolar value. These highly potent ligands were applied for characterization of strong PPIs between heteromers of PKA holoenzyme. The high affinity of 5-TAMRA functionalized ARC-1413 towards PKAc (K_d = 5 pM) allowed accurate determination of affinity of PKA subunits. The disruption of PKA holoenzyme was confirmed by a decrease in FRET between genetically engineered PKA subunits after supplementing the bifunctional ligand ARC-1411. Described technique is a promising approach for disruption of strong PPIs that possess too high binding energy to be cleavable in presence of monofunctional ligands.

2. LITERATURE OVERVIEW

2.1. Proteins

The ultimate regulators of living organisms are nucleic acids, their translation products, proteins have a broad variety of functions and can be more difficult to address in the sense of modeling, predicting, and analyzing. Proteins are polymers of amino acid (AA) residues that constitute 100–300 g/L (approximately 4 mM) of an eukaryotic cell (Theillet *et al.* 2014).

The sequence of AA residues (primary structure) in a protein is determined by a set of codons, triplets of mRNA nucleotides. The primary structure of a specific protein dictates its secondary, tertiary, and quaternary structures (Anfinsen 1973). Comprehension of protein folding is of paramount importance to understand biological processes. Folding of a protein through interactions between AA residues is described as a "hierarchical process", in which an unfolded translated protein possesses nucleation centers that form local segments (α-helixes, β-sheets, etc) and grow until protein has reached a native conformation (Honig *et al.* 1976). Aside this well-known basic principle, the exact understanding of and mechanical modeling to predict folding and subsequent importance in the biomolecular system has been challenging.

Developments led to the introduction of WSME model in 1990-s (Wako and Saito 1978; Muñoz and Eaton 1999). With two assumptions, this model calculates free-energy landscape for a protein, giving numerical values for the folding of N-terminal and C-terminal halves of the respective protein. WSME model explains many aspects of AA sequence structure arrangements relatively well, involving pathways of folding and unfolding, positioning of each constituent AA, and minimum energy of the native state. More importantly, this model can also account for multi-domain proteins and kinetic parameters of folding (Inanami *et al.* 2014). There are methods capable of recording protein folding experimentally, such as fluorescence techniques, IR, NMR, and CD (Buchner *et al.* 2011), which use is often limited by complexity and throughput of the assay. The kinetic characterization of folding for a significant portion of the whole human proteome with over 17 000 known proteins and few thousand missing proteins (Kim *et al.* 2014; Baker *et al.* 2017) with theoretical calculations is, therefore, more realistic in the near future compared to experimental techniques. The general understanding is that secondary structure elements and single-domain proteins fold with a limited speed (1 μs) and follow a simple equation $N/100$ μs, with N being the number of AA residues (Kubelka *et al.* 2004). Multi-domain proteins tend to show longer folding times, as the maturation of full structure involves the achievement of energetic minimum of an ensemble of constituents (Arai *et al.* 2011).

Making general assumptions about the specific protein can lead to a drastic error, as even some globular proteins fold in minutes and tens of minutes (Finkelstein *et al.* 2017). Physically prolonged folding times of proteins contradict to the overall efficiency of cellular operations, for example, even the

translation of an average protein (440 AA) in eukaryote completes in 1–2 minutes (Újvári *et al.* 2001).

2.1.1. Interactions between proteins

Correctly folded protein can subsequently contribute to the normally functioning cycle of a living cell. Without interactions between proteins, termed as protein-protein interactions (PPIs), the cellular signaling, and consequently cell-based life-forms, would not exist. The collection of PPIs is referred to as the interactome. According to human proteome, the human interactome is estimated to consist of 280 000 PPIs (Chatr-Aryamontri *et al.* 2015), out of which only 14 000 interactions have been confirmed experimentally (Rolland *et al.* 2014). Excluding internal interactions (intra-domain and domain-domain within one primary sequence), PPIs can be divided into four general categories: homo-obligomers, homo-complexes, hetero-obligomers, and hetero-complexes (Ofran and Rost 2003). *Obligomers* refer to obligatory or permanent interactions that rarely participate in signaling, *complexes* denote transient PPIs that are responsible for signal transduction (Ofran and Rost 2003). The majority of information is transferred specifically through interactions of hetero-complexes. Interfaces between proteins are formed preferably by hydrophilic AA residues (Arg, Asn, Gln, His), with the exception of hydrophobic Tyr residue, and the buried areas comprise hydrophobic residues (Ile, Val, Leu, Phe) (Yan *et al.* 2008). The contact area of PPIs spans a wide range from 300 to 3500 $Å^2$. There is little to no correlation between the strength and size of PPIs, as the dissociation constant of the complex has been shown to range from 10 μM to 100 pM for similarly sized (1500 $Å^2$) interfaces (Chen *et al.* 2013). Importantly, a major part of the interaction strength is caused by only a fraction of AAs of the interface termed "hot spots". This was demonstrated for the interaction between human growth hormone (hGH) and its receptor, in which 11 AAs contributed more than 4.18 kJ/mol and two AAs more than 16.7 kJ/mol into (negative) binding free energy out of 30 AAs at the interface (Clackson and Wells 1995).

A systematically studied and diverse PPI partner is SRC homology domain 2 (SH2). SH2 is conserved in 111 proteins. It is essential in mediating insulin and growth factor signaling (Liu *et al.* 2011). K_D values range from sub-nanomolar to sub-millimolar values for PPIs between SH2-comprising proteins and receptors (Liu *et al.* 2012).

In addition to folded proteins, the importance of intrinsically unstructured proteins (IUPs) in the PPI context has become evident (Dyson and Wright 2005). These proteins can exist under physiological conditions without any secondary structure or contain unstructured regions. Database of protein disorder (DisProt.org, accessed 01.06.2017) currently reports 557 eukaryotic proteins with unstructured regions, which range from tens to hundreds of AAs (Piovesan *et al.* 2017). Binding of IUP to its target protein can inhibit or induce

structural changes to the target or IUP itself. An example of fully IUP is the kinase-inducible domain (KID, gene name CREB1) when not bound to its target, cAMP-response-element-binding protein (CREB) binding protein (CBP) (Sugase *et al.* 2007). KID is a 341 AA long unstructured protein, which binds to KIX domain on CBP with a K_D of 1.5 μM, accompanied by the formation of two α-helixes within its structure (Sugase *et al.* 2007). CBP is a large (2442 AAs) and exemplary protein with numerous PPIs, while up to 50% of CBP itself is unstructured (Dyson and Wright 2005). In the case of oxygen deficiency, hypoxia-inducible transcription factor 1α (HIF1α) winds tightly around transcriptional-adaptor zinc-finger (TAZ) domain 1 within CBP (Dames *et al.* 2002). This strong interaction (K_D = 7 nM) is possible due to the loose nature of both partners, which would require a larger interaction area for two globular structured proteins. In this regard, a disorder in the protein structure in complex living organisms allows stronger interactions at the lower mass of proteins, estimably resulting in 15–30% smaller cellular volume (Gunasekaran *et al.* 2003).

2.1.2. Post-translational modifications

In addition to approximately 20 000 human protein-coding genes, alternative splicing and post-translational modifications may altogether result in millions of different protein variants (Jensen 2004). There are over 100 different modifications that have specific outcomes for specific proteins, such as protein localization or folding and subsequent participation in PPIs (Khoury *et al.* 2011). A single protein may be subjected to numerous post-translational modifications simultaneously. For example, the functioning of HIF1α is regulated by 17 post-translational modification sites according to UniProt database (UniProt.org, accessed 01.06.2017), six of which are targets of phosphorylation, two sites are prone to SUMOylation, and three for ubiquitination. Phosphorylation is the most frequent and universal post-translational modification in the biological kingdom (Beltrao *et al.* 2013).

2.2. Protein kinases

The superfamily of protein kinases with over 500 members is one of the largest in the set of mapped human protein-coding genes (Manning 2002). Protein kinases are transferases that functionalize target proteins with phosphoryl groups from nucleotides. Phylogenetically, protein kinases are divided into seven main groups: AGC (PKA, PKC, PKG, and ROCK families), CAMK, CMGC, CK1, STE, TK, and TKL.

According to experimental data, over 10 000 proteins in human proteome are phosphorylatable, with a total of 86 000 phosphorylation sites (Vlastaridis *et al.* 2017). The vast importance of correct phosphorylation in sustaining normal

signaling means that aberrant functioning of protein kinases entails health disorders. The dysfunctional activity of protein kinases has been linked to a number of diseases, from diabetes to neurological diseases and cancer (Arencibia *et al.* 2013).

2.2.1. cAMP-dependent protein kinase

The catalytic subunit (PKAc) of cAMP-dependent protein kinase (PKA) is an extensively characterized member of the AGC-group kinases. Three genes, *PRKACA*, *PRKACB*, and *PRKACG* encode PKA catalytic subunit isoforms PKAcα, PKAcβ, and PKAcγ, respectively (Turnham and Scott 2017). Isoforms PKAcα and PKAcβ are expressed in various tissues, while PKAcγ is expressed only in testis. Reportedly, there is the fourth gene *PRKX* that leads to expression of PKAc isoform that is involved in neural development and sexual differentiation (Huang *et al.* 2016). While the primary sequence is only 48% similar to PKAcα, *PRKX* product exhibits extensively conserved sequences in catalytically important regions.

PKA activity is mostly regulated by the levels of the secondary messenger cAMP. Extracellular effectors activate adenylate cyclase (AC), which catalyzes ATP conversion to cAMP. At low cAMP levels, PKA exists as a holoenzyme comprising AKAP (A-kinase anchor protein)-bound PKA regulatory (PKAr) subunit dimer and two PKA catalytic (PKAc) subunits ($PKAr_2$:$PKAc_2$); activation of AC leads to elevated concentrations of cAMP, four cAMP molecules bind to the PKAr dimer and the resulting conformational change leads to release of two catalytic PKA subunits for phosphorylation of downstream targets (Taylor *et al.* 2004). Myristoylation at N-terminal glycine residue of PKAc can force its localization to the membrane, greatly reducing the diffusion of PKAc and supporting the phosphorylation of protein substrates, especially intracellular receptor sites (Tillo *et al.* 2017). As a negative feedback mechanism, PKAc activates phosphodiesterases (PDEs), for example, PDE4D3, which decrease cAMP concentration and promote the reformation on PKA holoenzyme (Terrin *et al.* 2012). However, in case PKAc is localized onto the membrane by myristoyl group, the slow escape or diffusion from the membrane to PKAr may greatly hinder the reduction of catalytic activity.

In addition to the release from the PKAr subunit, the catalytic activity of PKAc is possible only after two phosphorylation events within its structure: autophosphorylation at Ser338 and phosphorylation of Thr197 by PDK1. Two cAMP-independent PKA regulation pathways have been described: IκB interaction with PKAc and Smad4 binding to PKAr (Zhong *et al.* 1997; Zhang *et al.* 2004).

Free and catalytically active PKAc phosphorylates roughly 100 protein targets (Kreegipuu *et al.* 1998), including CREB for association with CBP. The activity in the cytosol is reduced by the decrease in cAMP levels, however, PKAc transported into the nucleus is bound by natural heat-stable protein kinase

inhibitor (PKI) (Chen *et al.* 2005). PKI binds to the substrate-binding site of PKAc, inhibiting the latter enzyme and transporting PKAc to the cytosol. Well-studied interactions involving PKAc give insight into numerous PPIs that participate in signaling cascade from the viewpoint of a single protein. Signaling cascade of PKAc can be modulated differently at each PPI intraface (interaction area of one protein partner in PPI), for example by targeting AKAP:PKAr or $PKAr_2$:$PKAc_2$. However, the disruption of PKA holoenzyme is a complicated task due to the strong PPI (K_D = 100 pM) between PKAr and PKAc subunits (Cheung *et al.* 2015).

2.2.2. Rho-associated protein kinase

Rho-associated protein kinase (ROCK) is a ubiquitously expressed kinase in human organism that belongs to the AGC-group of protein kinases. ROCK has two isoforms: ROCK1 and ROCK2 with molecular weights of 158 kDa and 161 kDa, respectively. The protein with high molecular weight incorporates several domains: kinase domain in the N-terminus, coiled-coil domain, Rho-binding domain, and pleckstrin homology (PH) domain in the C-terminus (Leung *et al.* 1995; Jacobs *et al.* 2006). ROCK isoforms do not specifically require any posttranslational modifications in kinase domain for catalytic activity. Instead, phosphorylation by ROCK is regulated by Rho-binding and PH domains, which interact with and autoinhibit the kinase domain. Binding to Rho-GTPases (Rho, CDC42, etc.) alters the conformation of ROCK: Rho-binding domain interacts with membrane-associated Rho-GTP, PH domain binds to negatively charged lipids, and hydrophobic motif within the kinase domain enforces two ROCK subunits to form a dimer (Pearce *et al.* 2010). Triggered conformational change activates ROCK for downstream signaling.

Phosphorylation of over 30 substrates by ROCK regulates cytoskeletal dynamics and morphology/contraction of a cell (Schofield *et al.* 2013). Well-studied target myosin-binding subunit (MYPT1) phosphorylation at Thr696 and Thr855 is mediated by ROCK, which leads to MYPT1 dissociation from myosin light chain phosphatase (MLCP) (Loirand and Touyz 2015). Myosin light chain can bind to actin filament after phosphorylation by myosin light chain protein kinase (MYLK), resulting in muscle contraction (Stull *et al.* 2011).

2.2.3. RAC Ser/Thr protein kinase

RAC serine/threonine protein kinase (PKB, also known as Akt) isoforms PKBα, PKBβ, and PKBγ are expressed in numerous human tissues (Petryszak *et al.* 2016). Similarly to ROCK, PKB incorporates a PH domain. PH domains of PKB have been found to interact with T-cell leukemia/lymphoma 1 (TCL1) oncoprotein, resulting in increased PKB activity, and inosine-5'-monophosphate dehydrogenase (IMPDH), leading to increase in IMPDH enzymatic activity

(Brazil *et al.* 2002). The central importance of PH domain lies in its interactions with phosphatidylinositol-3,4,5-triphosphates and promotion of PKB localization onto cell plasma membrane (Yang *et al.* 2002). Membrane-association is necessary for subsequent phosphorylation of PKB at Thr305/308/309 residues by phosphoinositide-dependent-kinase-1 (PDK1) (Alessi *et al.* 1996). Full activation of PKB requires phosphorylation at Ser473/475/576 residues by the mammalian target of rapamycin (mTOR) (Sarbassov 2005; Alessi *et al.* 1996).

The substrate consensus sequence of PKB lacks conformity as the only regularity between numerous substrates is Arg in position –3 from phosphorylation site of Ser/Thr (Brazil and Hemmings 2001). Substrates phosphorylated by PKB are key regulators of cell survival, proliferation, and growth, including Bcl-2-associated death promoter (BAD), thereby preventing the cell from entering programmed cell death, and glycogen synthase kinase 3 (GSK3), which is inactivated for glycogen production (Shaw *et al.* 1997; Datta *et al.* 1997).

2.3. Ligands

Detailed understanding of protein structure and interactions in signaling pathways has enabled the construction of molecules with remarkable affinity and selectivity towards the target for influencing, in most cases, inhibiting a specific process. Lead molecules are studied and subjected to modifications, and promising candidate molecules are meticulously characterized biochemically, *in vitro*, *in vivo*, and in clinical trials. Only a few candidates succeed to comply with the requirements in clinical trials and can be marketed as drugs. Currently, 82.4% of marketed drugs are distributed amongst 8 protein family classes: 7-transmembrane family 1 (30.3%), nuclear receptors (13.5%), voltage-gated ion channels (8.0%), reductases (7.6%) ligand-gated ion-channels (7.0%), electrochemical potential-driven transporters (6.9%), kinases (5.9%), and proteases (3.4%) (Santos *et al.* 2016). Compounds targeting kinases and proteases make up 8.3% of the drugs, however, their clinically non-approved inhibitors in European Bioinformatics Institute (ChEMBL) database form up to 27.2% of compounds and protein kinase-targeting drugs approved between 2011–2015 constitute 28% of all approvals (Santos *et al.* 2016).

In 1997, Lipinski *et al.* analyzed the structures of approved drugs and postulated "*The Rule of Five*" to aid the rational design and discovery of novel candidates for oral drugs (Lipinski *et al.* 1997). According to these rules, a molecule possessing more than five hydrogen bond donors and ten hydrogen bond acceptors, molecular weight over 500 Da, and octanol-water partition coefficient (log *P*) over five is less likely to permeate cell plasma membrane and should not proceed into clinical trials. These rules were insightful and helped to avoid failures in later stages of drug development, however, new knowledge acquired within two decades has made it clear that many complex diseases need a different approach for successful treatment. For example, some

drug candidates in clinical trials greatly exceed the molecular weight limit of 500 Da (Agarwal *et al.* 2014).

The first requirement of a promising lead molecule is sufficient affinity towards its target. The affinity or interaction strength is expressed as equilibrium dissociation constant (K_D) of the complex between target protein and inhibitor (Equation 1A).

A

$$K_D = \frac{[P][I]}{[PI]}$$

B

$$\ln K_D = \frac{\Delta G_B^0}{RT} = \frac{\Delta H_B^0 - T\Delta S_B^0}{RT}$$

Equation 1. A) K_D, the equilibrium dissociation constant of a complex between protein and inhibitor; $[P]$, the equilibrium concentration of free protein; $[I]$, the equilibrium concentration of free inhibitor; $[EL]$, the equilibrium concentration of protein:inhibitor complex. B) ΔG_B^0, standard free energy change of the binding between protein and inhibitor; R, ideal gas constant; T, absolute temperature; ΔH_B^0, standard enthalpy change of binding; ΔS_B^0, standard entropy change of binding.

K_D of the complex decreases with increasing strength of the interaction. K_D can be related to standard free energy change of binding, ΔG_B^0 (opposite sign to ΔG^0) (Equation 1B) that comprises both enthalpic (ΔH_B^0) and entropic (ΔS_B^0) change upon binding (Du *et al.* 2016). Decreasing ΔG_B^0 and therefore K_D is possible by strengthening interactions (negative ΔH_B^0) or inflicting disorder within protein or environment (positive ΔS_B^0) upon binding. However, inhibitor with very strong interaction consequently brings along structural order and loss in degrees of freedom within protein and optimizing both ΔH_B^0 and ΔS_B^0 is frequently conflicting. Most of the inhibitors are enthalpy-driven, as the hydrogen-bond interactions are easily predicted and calculated based on available crystal structures of proteins (Olsson *et al.* 2008). In the later stages of drug development, inhibitors can be designed structurally more rigid to increase ΔS_B^0 and gain in overall affinity, while retaining strong interactions.

2.3.1. Kinetics of ligand:protein complexes

The association and dissociation rate constants between a ligand and a protein are important parameters that are often overlooked in biochemical characterization of interactions. The association rate constant (k_{on}) describes the speed of colliding and complex formation between two molecules according to the rate of second-order reaction ($M^{-1}s^{-1}$). The dissociation rate constant (k_{off}) describes the break-up of a complex, mostly following the rate of a first-order reaction (s^{-1}). Kinetic parameters are directly related to K_D according to Equation 2A. However, in most cases with biomolecular targets, the interaction can be divided into two distinct steps: formation or breakdown of initial complex, and conformational change (induced fit) of protein (Meyer-Almes 2015).

A $$K_{\mathrm{D}} = \frac{k_{\mathrm{off}}}{k_{\mathrm{on}}}$$ **B** $$k_{\mathrm{off}} = \frac{1}{\tau}$$

Equation 2. A) k_{off}, dissociation rate constant of ligand:protein complex; k_{on}, association rate constant of ligand:protein complex; B) τ, the residence time of the complex.

Structure-affinity relationship (SAR) studies of lead compounds were mainly focusing on K_{D}, omitting the possibility to steer the selectivity towards the desired target by increasing residence time (Equation 2B). After the introduction of the term and its importance, improving the residence time of a ligand on its target has become a widely accepted strategy (Copeland *et al.* 2006). The prolonged residence time of a ligand towards specific target compared to off-target proteins results in improved outcome in a complex system (*e.g.*, cellular environment), as the ligand is kinetically occupied in complex with the target. In parallel, drug molecule binding to and quickly dissociating from off-target results in alleviated toxic effects (Lu and Tonge 2010). A successful example is Gleevec (Imatinib), the first selective cancer therapeutic for Tyr-protein kinase Abl (Manley *et al.* 2002). Kinetic analysis revealed that although Abl and protein kinase Src share almost identical binding site, the residence time of Gleevec on Abl is 60-fold greater compared to Src (Agafonov *et al.* 2014).

2.3.2. Monofunctional ligands

In the current context, monofunctional ligand is referred to as a molecule which occupies a single distinct region on a protein. In most cases, ligands behave as inhibitors for disruption of the interaction between protein and its substrate, while the development of stabilizers of PPIs has the reciprocal purpose of reinforcing the interaction. Depending on the mechanism of action, monofunctional ligands can be divided into a variety of groups, not all of which are discussed here.

Covalent or irreversible monofunctional ligands bind to and form a covalent bond with the target protein. Covalent modification is usually accompanied with long inhibition of the natural action of the protein. An early successful example of this approach is the use of acetylsalicylic acid which suppresses inflammation by acetylating prostaglandin-endoperoxide synthase (PTGS), despite that the approval for its use as a drug preceded the resolving of the exact mechanism by 85 years (Roth and Majerus 1975). Extensive research on covalent inhibitors of protein kinases has largely been unfruitful due to the conserved kinase site within kinome. An irreversible Bruton tyrosine kinase (BTK) inhibitor is a successful example that targets uncommon binding site holding a cysteine residue (Cys481), granting higher selectivity (Honigberg *et al.* 2010). Ibrutinib has been approved for therapeutic use in rare lymphoma, Waldenström macroglobulinemia, in which

BTK is constitutively active and contributes to the suppression of apoptosis-induced cell death (Abeykoon *et al.* 2017; Yang *et al.* 2013).

Reversible monofunctional ligands form a transient non-covalent interaction with the target protein. These inhibitors can bind directly to the interaction site (active site of the enzyme) or allosteric site. The comprehensive understanding of PPI interfaces and signaling pathways has only recently increased the systematic study of inhibiting PPIs. The potency of small molecules for binding PPI interfaces is usually small, restricted by physical limitations to molecular weight compared to large interaction area between the interacting proteins. For example, most small molecules have a micromolar affinity for disruption of PPI between specific SH2-domain and receptor, while inhibitors targeting specific SH2 interactions achieve low-nanomolar affinity (Kraskouskaya *et al.* 2013). An emerging role in targeting PPIs is the stabilization of the interaction by ligand-binding. This mechanism has been successfully demonstrated with compound RO-2443 on double minute 2 (MDM2) and double minute 4 (MDM4) interaction. RO-2443 binds into the interface MDM2/MDM4 and stabilizes the interaction, preventing the protein complex from rearranging and ubiquitinating tumor suppression antigen p53 by the really interesting new gene 1 (RING1) domain, promoting apoptosis of cancer cells (Graves *et al.* 2012).

A protein kinase has two substrates: a nucleotide, typically ATP, and a protein. Reversible monofunctional inhibitor competitive with ATP has to overcome millimolar intracellular concentration of the latter compound (Ataullakhanov and Vitvitsky 2002; Knight *et al.* 2007). Regardless, the growing number of cancer incidences has driven the inevitable need for its chemotherapy. Protein kinases are obvious inhibition targets due to their role in aberrant signaling in cancer cells and currently, 23 out of 28 FDA-approved small-molecule protein kinase drugs are reversible ATP-competitive inhibitors (Wu *et al.* 2016). Half of these drugs also bind an adjacent site simultaneously with the ATP-site, but no drugs are available for remote allosteric sites of protein kinases. In contrast, protein substrate-competitive monofunctional inhibitors have the potential to achieve high selectivity. However, protein substrate-competitive inhibitors target less defined binding site over the large surface area, resulting in too low affinity for sufficient efficacy *in vivo* or fail to cross cell plasma membrane due to high molecular weight and polarity (Bogoyevitch *et al.* 2005).

2.3.3. Bifunctional ligands

Bifunctional ligands that target proteins are generally reversible and occupy two distinct regions of the protein simultaneously. These regions may be identical, if located on separated proteins a protein homodimer is formed (Zhou *et al.* 2008). However, most bifunctional ligands for binding proteins are heterobifunctional and designed for inducing the formation of protein heterodimers and thereby trigger a subsequent biological response (Corson *et al.* 2008). The interactions

within triple (ternary) complex composed of two proteins and a bifunctional ligand may be reinforced by the effect from avidity and favorable contacts between proteins (Vauquelin and Van Liefde 2012; Zhou *et al.* 2008).

The application of bifunctional inhibitors has been mostly studied for dimerization or stabilization of protein complexes (Spencer *et al.* 1993) and less research has been described related to their application for disruption of PPIs. A successful example is a bifunctional ligand consisting of two pentapeptides linked by PEG that bind to postsynaptic density protein 95 (PSD95) domains PDZ1 and PDZ2 (Bach *et al.* 2012). This disrupts the PSD85 interaction with both NMDA ionotropic receptor and nitric oxide synthase (nNOS), inhibiting the generation of nitric oxide and protecting cells from the damage.

Successful construction of bifunctional ligands to target protein kinases was first reported for PKC (Ricouart *et al.* 1991). In the case of protein kinases, heterobifunctional inhibitor occupies both the hydrophobic ATP-pocket and protein substrate-binding site on a single target protein simultaneously. A common approach for designing a bifunctional ligand is the conjugation of two moieties with known binding characteristics by a linker unit (Loog *et al.* 1999; Parang *et al.* 2001). Extensive structure-affinity research (SAR) and co-crystal analysis of adenosine analogues and arginine-rich peptide conjugates (ARCs) highlighted the importance of linker region between two moieties (Lavogina *et al.* 2010a; Pflug *et al.* 2010). The optimal length of the linker leads to substantial increase in affinity and offers the possibility to improve selectivity towards target protein. The binding free energy of a bifunctional ligand with its target protein is the sum of binding free energies of two interacting moieties plus an additional gain from $\Delta S_{\mathrm{B}}^{0}$ of adjoining two moieties (Jencks 1981).

2.4. Methods for studying protein kinases, protein-protein interactions, and inhibitors

2.4.1. Protein kinase activity assays

The activity of a protein kinase is measured by the rate at which its substrate is phosphorylated, corresponding to the *enzyme unit* (U), where 1 U equals the amount of protein kinase that phosphorylates 1 nanomole of the specific substrate within 1 minute at 30 °C (Hastie *et al.* 2006). Instead of physiological substrates, a phosphorylatable peptide sequence mimicking the substrate can be used (Macala *et al.* 1998). The classical method for assessing the activity is based on monitoring the migration of substrates, radioactively labelled ^{32}P-ATP and peptide substrate on phospho-cellulose paper (Witt and Roskoski 1975). The high risk related to radioactive samples led to chromatography methods based on fluorophore-conjugated substrate peptides (Viht *et al.* 2005). Activity profiling has also been demonstrated in a high-throughput system with nanoliter volumes but is limited to glycerol-presence and substrate-product conversions that incorporate a large Stokes shift (Ma *et al.* 2005). In these activity assays,

one substrate is taken in excess and phosphorylation rate is monitored in time (Scheme 1A). The equation describing the resulting pseudo first-order reaction (Scheme 1B) is further simplified by Michaelis-Menten equation (Scheme 1C), where $V_{max} = k_{cat}[E]_t$ and $K_M = \frac{k_{-1} + k_{cat}}{k_1}$. Each of these assays can be used for characterization of inhibitors, where the assay is repeated in the presence of various concentrations of the inhibitor (Scheme 1A).

A

$$\begin{array}{l} E + S \underset{k_{-1}}{\overset{k_1}{\rightleftarrows}} ES \xrightarrow{k_{cat}} E + P \\ + \\ I \\ k_{on} \downarrow\uparrow k_{off} \\ EI \end{array}$$

B

$$v_0 = \frac{k_{cat}[E]_t[S]}{\frac{k_{-1} + k_{cat}}{k_1} + [S]}$$

C

$$v_0 = \frac{V_{max}[S]}{K_M + [S]}$$

Scheme 1. A) The monosubstrate reaction mechanism in the presence of competitive inhibitor: k_{cat}, the rate constant of product formation; k_1, the association rate constant; k_{-1}, dissociation rate constant; *E*, enzyme; *S*, substrate; *P*, product; *I*, inhibitor. B) Equations for the rate of monosubstrate reaction: v_0, initial velocity; $[E]_t$, the total concentration of enzyme; [S], the concentration of substrate. C) Michaelis-Menten equation: K_M, Michaelis-Menten constant; V_{max}, the maximum rate of substrate conversion.

Binding assays are a convenient alternative to monitoring substrate phosphorylation. Instead of application of two substrates, binding of the ligand to the catalytically active enzyme is employed. The unlabeled ligand can be used in heterogeneous biosensor assays, such as surface plasmon resonance (SPR) (Viht *et al.* 2007). SPR provides kinetic parameters in addition to the value of K_D. A sensitive homogeneous setup requires the conjugation of the ligand with a fluorophore, resulting in a fluorescence probe suitable for use in various FI-based assays that differentiate between the free probe and probe:enzyme complex. Methods with fluorescence polarization/anisotropy (FP/FA) read-out can be used for measurement of both direct binding of the probe to the enzyme and displacement of the probe from the complex with a protein by an inhibitor (Owicki 2000). The FP and FA are interchangeable quantities, while the usage of FA is preferred as it accounts for total intensity (Equation 3).

A

$$P = \frac{I_{||} - I_{\perp}}{I_{||} + I_{\perp}}$$

B

$$r = \frac{I_{||} - I_{\perp}}{I_{||} + 2I_{\perp}}$$

Equation 3. *P*, polarization; $I_{||}$, emission intensity parallel to incident light; $I_{\perp}$, emission intensity perpendicular to incident light; *r*, anisotropy.

FA assay is based on the difference of rotational speed of the free and protein-bound fluorescent probe. Polarized excitation of free fluorescent probe rotating rapidly results in depolarization of emitted light, leading to decrease in $I_{\parallel}$ and low anisotropy value; upon binding to a target protein, rotation of fluorescent probe is hindered and anisotropy increases (Lakowicz 2006a). Despite the simplicity of FA assay, the affinity of fluorescent probe limits the highest affinity of competitive inhibitor under observation and the lowest concentration of the target protein (Huang Xinyi 2003).

2.4.2. Protein interaction analysis

Information regarding PPIs can be extracted using multiple methods that differ greatly in their nature. Each method has specific benefits and drawbacks, requiring the need for confirming the result in parallel by another method. Simple and low-cost option for discovering PPIs has been yeast two-hybrid (Y2H) assay.

Y2H is a genetic method, in which transcription factor is split and fused separately with two proteins under observation, activating reporter gene if the two proteins interact (Fields and Song 1989). Despite aiding in the discovery of many PPIs, Y2H is prone to false-positives and does not describe mammalian interactome well with estimation of only 10 000 interactions (Sprinzak *et al.* 2003).

Co-immunoprecipitation (co-IP) technique is based on pull-down of antigen proteins onto the antibody-functionalized support and subsequent elution for analysis (Ren *et al.* 2003). Co-IP may detect protein complexes composed of many proteins and prepared surface can be used in multiple experiments. The analysis is limited to the specific antigen, making co-IP a good method for validation of interactions, but impractical for whole interactome analysis (Markham *et al.* 2007). Therefore, attention has been turned to simple native gel-electrophoresis (NE) to address the difficulties related to the PPI discovery in a universal manner (Camacho-Carvajal *et al.* 2004). For example, whole cell lysate is introduced to mild conditions that retain stable PPIs and the proteins co-migrate in an electric field. Optimized NE method is also capable of analyzing membrane protein interactions (Wittig and Schägger 2009).

Y2H, co-IP, and NE techniques are frequently combined with mass-spectrometry (MS), which provides structural details (primary AA sequence) about the separated proteins or protein complexes (Farmer and Caprioli 1998). MS has been developed into highly capable technique for discovering PPIs from living cells by chemical cross-linking, subsequent cell lysis, proteolysis, and comparison of detected peptides against the database (Zhang *et al.* 2009).

Lately, nuclear magnetic resonance (NMR) has been demonstrated as a perspective technique for characterization of PPIs. Compared to the capability of NE for detecting stable (K_D < 1–10 μM) PPIs, a solution NMR can

additionally visualize transient (K_D > 1 μM) PPIs, which for most methods are kinetically too labile to detect (Liu *et al.* 2016).

PPIs that have been confirmed can be further characterized by using Förster-type resonant energy transfer (FRET) phenomenon, in which interacting partners are fused with fluorescent proteins or chemical labels (Scheibner *et al.* 2003; Mitra *et al.* 1996). FRET occurs between excited donor (D) molecule and ground-state acceptor (A) molecule as a non-radiative energy transfer, as revealed by the decrease of fluorescence intensity in the donor channel and its increase in acceptor channel (Lakowicz 2006b). FRET provides information regarding cellular localization and the dynamics of interacting partners in response to extracellular stimuli.

Isothermal titration calorimetry (ITC), similarly to FRET, can be used for gaining further information regarding known interactions. ITC is a widely applied technique for obtaining thermodynamic information about two interacting partners, affording the determination of stoichiometry, ΔG_B^0, ΔH_B^0, and ΔS_B^0 (Perozzo *et al.* 2004). Downsides of the ITC method are the requirement of large amounts (more than nanomoles) of reagents and its inaccuracy if determining very strong interactions (<10 nM) (Wiseman *et al.* 1989).

3. AIMS OF THE STUDY

Protein kinases, as well as protein-protein interactions, participate in almost every aspect of intracellular signaling. It is therefore well known and understandable that aberrant functioning of protein kinases may lead to a plethora of diseases, many of which tend to be difficult to alleviate or cure. Nevertheless, the research to modulate the activity of known disease-related protein kinases is intensifying and drug discovery process can benefit from novel sophisticated assays and strategies.

This study focused on the development and characterization of biligand-derived photoluminescence probes for highly sensitive assays for basophilic protein kinases. The main tasks that were addressed in the present study were the following:

- Application of protein kinase binding-responsive ARC-Lum(Fluo) probes for analysis of the binding kinetics of inhibitor:protein kinase complexes.
- Construction of high-affinity bifunctional ARC-type inhibitors by reference to results of extensive structure-affinity studies and X-ray analysis of ARC:protein kinase co-crystals.
- Application of bifunctional ARC-type inhibitors for disruption of strong protein-protein interactions.
- Clarification of the competitive ligand-facilitated dissociation mechanism of the bimolecular complex between a bifunctional ligand and protein kinase.

4. MATERIALS AND METHODS

4.1. Binding and displacement assays

4.1.1. Time-resolved measurement of luminescence intensity

Time-resolved (TR) measurement of luminescence was performed in an assay buffer (if not noted otherwise) consisting of 50 mM HEPES hemisodium salt (Sigma or Santa Cruz) (pH = 7.5), 150 mM NaCl (Riedel-de Haën), 0.5 mg/mL BSA (Sigma), 5 mM dithiothreitol (Sigma), and 0.005% P20 polysorbate (Sigma) with final sample volume of 20 µL. Biochemical measurements for obtaining the activity of protein kinases and the affinities of competitive inhibitors were conducted on black nonbonding 384-well microplates (round-bottom low-volume wells, codes 3676 or 4514). The microplates and sample solutions were preincubated and measured at 30 °C.

PHERAstar platereader (BMG Labtech) was used for measurement of luminescence intensity. Optical modules HTRF 802D1 [EX 337(50) nm, EM 675(50)/620(20) nm] or TRF 904B1 [EX 337(50) nm, EM 590(50)/545(10) nm] were used to filter out respective wavelengths. The luminescence signal was registered in time-gated mode (60 µs delay time after irradiation, 150 µs or 400 µs intensity acquisition interval).

The concentration of the active protein kinase was determined by preparation of two- or three-fold dilution series of protein kinase and the addition of luminescent probe [ARC-Lum(Fluo)] at fixed concentration in the assay buffer (binding assay). Luminescence intensity was measured after incubation for 15 min and results were fitted in GraphPad Prism 5.0 (GraphPad Software) with non-linear regression (Equation 4).

$$LI = B + M\frac{\left[L + K_{\mathrm{D}} + kE_0 - \sqrt{(L + K_{\mathrm{D}} + kE_0)^2 - 4LkE_0}\right]}{2}$$

Equation 4. E_0, nominal total concentration of the protein kinase; *LI*, luminescence intensity at E_0; *B*, background signal; *M,* molar luminescence intensity of ARC-Lum(Fluo) in complex with protein kinase; *L*, total concentration of ARC-Lum(Fluo); K_{D}, equilibrium dissociation constant between ARC-Lum and protein kinase; *k*, the ratio of active concentration to the nominal concentration of the protein kinase.

The affinity of competitive inhibitor was determined by preparation of three-fold dilution series of the inhibitor and addition of fixed concentration of a complex between protein kinase and ARC-Lum(Fluo) (displacement assay). Luminescence intensity was measured after incubation for 60 min and the results were fitted to a sigmoidal dose-response model. The resulting IC_{50} values were used to calculate displacement constants (K_{d}) according to Equation 5 (Nikolovska-Coleska *et al.* 2004).

$$K_{\mathrm{d}} = \frac{[I]_{50}}{\frac{[L]_{50}}{K_{\mathrm{D}}} + \frac{E_0}{K_{\mathrm{D}}} + 1}$$

Equation 5. $[I]_{50}$, the concentration of free inhibitor at 50% of displacement; $[L]_{50}$, the concentration of free ARC-Lum at 50% of displacement.

4.1.2. Förster-type resonant energy transfer (FRET)

Chinese hamster ovary (CHO) cells stably expressing C-terminally CFP-fused PKArIIβ and C-terminally YFP-fused PKAcα (C9H6) (Zaccolo *et al.* 2000; Lissandron *et al.* 2005) were seeded and grown for up to 72 h on a 6-well cell culture plate (Thermo Scientific, code 130184). Cell lysis was performed in NP-40 lysis buffer (Life Technologies, code FNN0021) in the presence of 1X protease inhibitor cocktail (Roche, Complete EDTA-free), 0.5 mM dithiothreitol, 1% Triton-X, and 0.5 mM phenylmethanesulfonyl fluoride. The approximate concentration of fused proteins in the cell lysate was estimated by the intensity of fluorescence in comparison to Alexa Fluor 488-conjugated ARC-679.

Solutions of inhibitors ARC-1411, ARC-902, and PKAc activator cAMP were prepared in three-fold dilution series in assay buffer without 5 mg/mL BSA. CHO cell lysate was added to a final dilution of 5% (n = 2). Fluorescence intensity was measured after 1 h incubation period at 30 °C using PHERAstar platereader and the optical module FI608A [EX 427(10) nm, EM 530(10)/480(10) nm]. The relative fluorescence intensity ratio (FI_{r}) was calculated from the results according to Equation 6.

$$FI_{\mathrm{r}} = \frac{I_{\mathrm{a}}}{I_{\mathrm{d}}} \Big/ \frac{I_{\mathrm{a,D}}}{I_{\mathrm{d,D}}}$$

Equation 6. I_{a}, emission intensity in the acceptor channel; I_{d}, emission intensity in the donor channel in the absence of a competitor, and $I_{\mathrm{a,D}}$ and $I_{\mathrm{d,D}}$ are the emission intensity in the acceptor and donor channel in the presence of the competitor, respectively. The concentration-dependent profile of FI_{r} was fitted to a sigmoidal dose-response model to find IC_{50} values.

4.2. Thermal shift assay

Thermal shift assay was performed in a buffer composed of 50 mM Tris (pH = 7.5) and 50 mM NaCl with a final sample volume of 25 µL. Protein kinase solutions were used at a fixed total concentration of 10 µM in the presence of Sypro Orange (90-fold dilution from 5000X DMSO stock, Thermo Scientific, code S-6650) with or without (control) 40 µM inhibitor. Samples were measured on Multiplate low-profile 48-well unskirted PCR plates (BioRad) covered with Microseal C Optical seals (BioRad) in MiniOpticon RT-PCR system (BioRad). The thermostat block was cooled to 5 °C and temperature

gradient was initiated with heating 1 °C/s up to 90 °C. The temperature gradient was accompanied with 0.3 s measurement intervals, in which samples were irradiated at 530 nm and the fluorescence intensity was registered at 560 nm. The resulting fluorescence intensity data was analyzed with Opticon Monitor software (BioRad). Protein melting temperature was determined as the highest ratio of $\frac{\Delta I}{\Delta T}$ during the temperature gradient, and confirmed by fitting the fluorescence intensity to the Boltzmann sigmoidal model (Equation 7):

$$FI = I_{\min} + \frac{I_{\max} - I_{\min}}{1 + e^{\frac{T_{50} - T}{a}}}$$

Equation 7. *FI*, fluorescence intensity at temperature *T*; I_{min}, fluorescence intensity at a lower plateau; I_{max}, fluorescence intensity at a higher plateau; T_{50}, the half maximal temperature of protein denaturation; *a*, slope tangential to the curve at T_{50}.

4.3. Dissociation kinetics assays

The kinetic characterization of dissociation of the complex of a protein kinase and ligand was performed in assay buffer (3.1.1.) on black round-bottom low-volume nonbonding 384-well microplates (code 3676 or 4514). The concentrations of ligands were determined spectrophotometrically using NanoDrop 2000c (Thermo Scientific) and concentration of the active form of protein kinase was determined as described in 3.1.1. All reagent solutions, spectrofluorometer, microplate, and pipette tips were preincubated at 30 °C on microplate thermostat (Thermo Scientific). Depending on the fluorescent reagent used, HTRF 802D1 [EX 337(50) nm, EM 675(50)/620(20) nm], TRF 904B1 [EX 337(50) nm, EM 590(50)/545(10) nm], or FI608A [EX 427(10) nm, EM 530(10)/480(10) nm] optical module was employed for registration of the signal intensity.

Two assay setups were used: the intensity decay of fluorescent complex was monitored by the addition of competitive inhibitor or non-fluorescent complex was disrupted by ARC-Lum(Fluo) probe and intensity increase was monitored. 10 µL solution of the competitive ligand was mixed with 10 µL solution of the complex on microplate at $t = 0$ and the signal intensity was registered in time with 5–60 s intervals. The resulting signal profile was analyzed with Equation 8A to find k_{off}. Equation 8B was subsequently used where necessary to correct the residence time (τ) for incomplete dissociation of the initial complex.

A

$$I = e^{-k_{\text{off}} \cdot t}\left(I_0 - I_{\text{plateau}}\right) + I_{\text{plateau}}$$

B

$$\tau = \frac{1}{k_{\text{off}} \cdot \frac{I_0 - I_{\text{plateau}}}{I_0}}$$

Equation 8. A) *I*, signal intensity at timepoint *t*; I_0, initial signal intensity; $I_{plateau}$, signal intensity at equilibrium. B) τ, the residence time of complex corrected according to incomplete dissociation.

4.4. Isothermal titration calorimetry

Untagged full-length human PKAc (UniProt accession no. P17612) was expressed in Escherichia coli BL21-(DE3) cells (Stratagene) from a construct based on the vector pET-28b(+) (Novagen) in Studier autoinduction medium. PKAc was purified as described previously (Engh *et al.* 1996). PKAc samples were previously dialysed overnight at 4 °C against buffer comprising 75 mM Tris (pH 7.5) and 20 mM NaCl using SnakeSkin dialysis tubing (Thermo Scientific, cut off: 10 000 MW), and concentrated by using a spin-column (MilliPore, 5 mL, cut-off: 10 000 MW) at 4000 RPM. Isothermal titration calorimetry (ITC) was performed using a low-volume ITC200 (MicroCal). Titrations were performed by injecting 20 consecutive aliquots (1.6 µL) of ligand solution (200 µM) into the ITC cell containing PKAc (20 µM) at 30 °C. The samples were stirred at 410 RPM. Twenty injections were separated by 150 s of equilibration. MicroCal ITC200 control software (v 1.26) was used for experiment design and the data were fitted using MicroCal ITC200 Analysis Software (v 7.2).

5. SUMMARY OF RESULTS AND DISCUSSIONS

5.1. Development and validation of photoluminescence-based assays (Papers I and III)

5.1.1. Discovery of long-lifetime luminescence of ARC-Lum probes

The literature review adverted to the importance of protein kinases in cellular signaling and their role in diseases. The conserved structure of kinase domain allowed the identification of 518 genes coding protein kinases in the human genome (Manning *et al.* 2002). Many signaling pathways have been established, however, cross-talk between the pathways complicates comprehensive understanding of the contribution of individual protein kinases. Reliable methods are still needed for monitoring the cellular activity of protein kinases and determination of inhibitory potency of compounds in cells. The enzymatic property of protein kinases has enabled the development of various assays based on inhibition of phosphorylation reaction for characterization of ligands (Zhang *et al.* 2015; Stenroos *et al.* 1998; Rininsland *et al.* 2004).

The extensive structure-activity studies and X-ray analysis of ARC:PKAc co-crystals have supported the construction of bifunctional inhibitors possessing sub-nanomolar affinity towards PKAc (Lavogina *et al.* 2009). Functionalization of ARCs with fluorophores resulted in high-affinity fluorescence probes (ARC-Fluo probes). The comparison between FA-based binding assay with conventional substrate phosphorylation assay gave an excellent linear relationship between K_d and IC_{50} values (Vaasa *et al.* 2009). The sub-nanomolar affinity of ARC(Fluo) fulfilled important requirements for an effective application in FA-based assays for analysis of protein kinases: the required concentration of an analyte for anisotropy change can be small and only active fraction of the protein kinase is detected, as the probe binds selectively to a catalytically active form of the enzyme. Unfortunately, anisotropy-based assays are sensitive to non-specific binding, restricting their use in crude lysate samples and for cellular applications.

A homogeneous method based on TR measurement of FRET efficiency has been demonstrated by using europium (Eu) cryptates as FRET donors in combination with fluorescent proteins as acceptors (Bazin *et al.* 2001). Eu-cryptate emission spectra are characterized by narrow peaks, allowing the performance of measurement at wavelengths where only the acceptor emits. This technique eliminates many shortcomings of FA and FRET assays by filtering out the auto-fluorescence of the sample, drastically reducing non-specific interferences and permitting measurements in crude samples. However, the drawbacks of the assay are the need for the antibody, derivatization of the substrate with biotin and fluorescent protein with streptavidin. Further developments led to inhibitors functionalized with an organic dye, removing the

need for the labelled substrate, while His-tagging of the protein and anti-His antibody were still needed (Figure 1A) (Lebakken *et al.* 2009).

Next, ARC-type probes were constructed for the development of a TR-FRET assay for analyzing protein kinases. ARCs possessing sub- to low nanomolar affinity towards many basophilic protein kinases constitute a set of binders whose derivatization with fluorophores leads to fluorescent probes for the construction of generic binding assays exploring low concentration of the probe and kinase. An ARC-inhibitor comprising 5-(2-aminopyrimidin-4-yl)thiophene-2-carboxylic acid (AMTH) within ATP-competitive moiety was synthesized and the terminal lysine was conjugated with Alexa Fluor 647 dye (ARC-1063). Anti-His antibody was labelled with Eu-cryptate and His-tagged protein kinase was used as the target. It was expected that upon excitation at 337(50) nm, the increase in long-lifetime luminescence at 670(50) nm is registered upon formation of the ternary complex. In the course of the measurements, titration of ARC-1063 with protein kinase increased long-lifetime luminescence signal in a concentration-dependent manner even in the absence of the donor, Eu-cryptate-comprising anti-His antibody (Figure 1B).

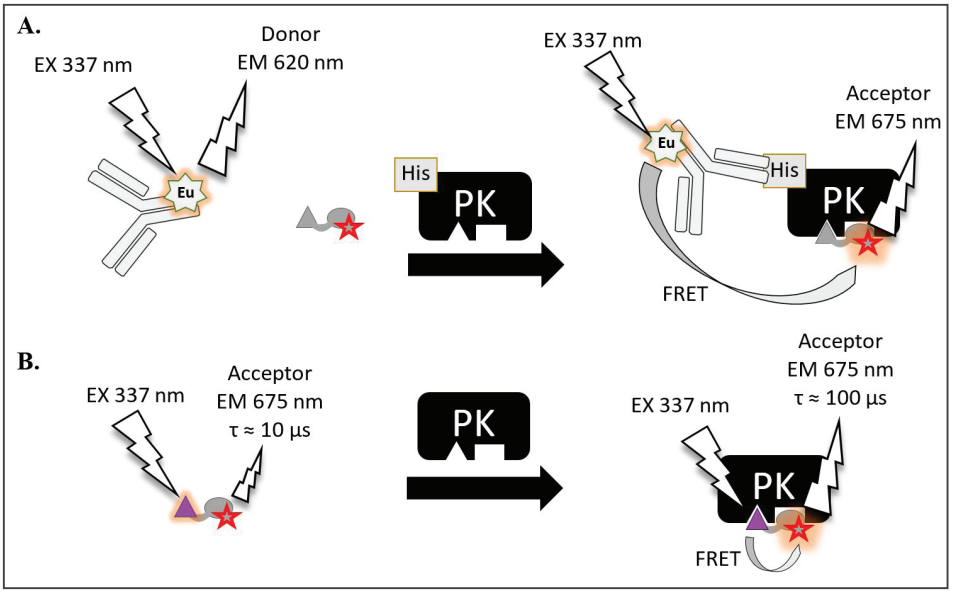

Figure 1. The difference between antibody:fluorescence ligand and ARC-Lum based homogeneous TR-FRET assays. A) FRET from the Eu-labeled antibody and fluorescence probe (FL) increases in ternary complex with a protein kinase (PK), accompanied by a decrease in the donor emission intensity (620 nm) and increase in the acceptor's emission intensity (675 nm). B) Excitation at 337 nm leads to long-lifetime luminescence intensity only if ARC-Lum probe is bound to a protein kinase.

Long-lifetime luminescence was characteristic for the complex of ARC-1063 with protein kinases PKAc, MSK1, ROCKII, PKBγ, PKGIα, and PKCδ, while in the absence of protein kinase the TR signal of luminescence of ARC-1063 was negligible (**Paper I** Figure 2A). A similar phenomenon was present with ARCs comprising 5-(2-aminopyrimidin-4-yl)selenophene-2-carboxylic acid (AMSE) within ATP-competitive moiety (ARC-1139). Furthermore, the heavy selenium atom induced greater long-lifetime luminescence intensity compared to sulfur-comprising π-conjugated fragment, and in parallel, shorter luminescence lifetime (**Paper I** Table 1). Titrating the complex of protein kinase and ARC-1063 or ARC-1139 with competitive inhibitor resulted in the concentration-dependent displacement of the probe, verifying the binding-responsive character of these probes. A novel property of organic long-lifetime luminescence probes was discovered and AMTH- or AMSE-comprising ARC-Lum probes (Figure 2) were introduced.

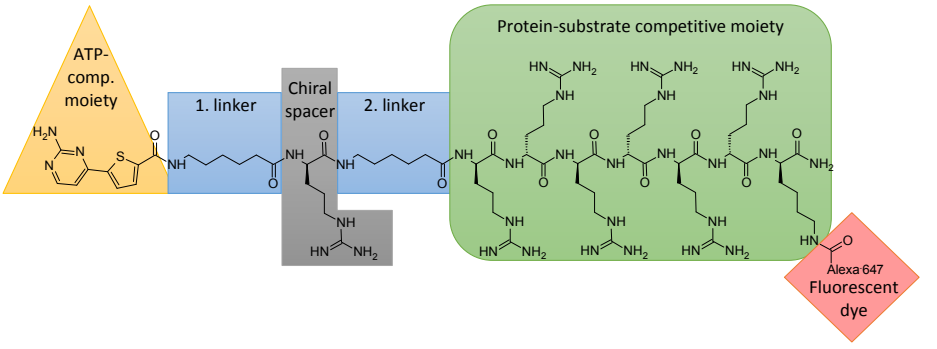

Figure 2. The structure of bifunctional probe ARC-1063. AMTH- or AMSE-comprising ATP-competitive moiety acts as an intramolecular, long-lifetime luminescence donor to the fluorescent dye.

The long-luminescence lifetime of ARC-Lum probes upon binding into the active site of protein kinase was attributed to the burial and fixation of the structure of ATP-competitive moiety into a deep hydrophobic pocket, which accompanies reduced quenching from dissolved oxygen species. Irradiating bound ARC-Lum excites the electron within AMTH- or AMSE-conjugated system (donor) into higher singlet energy state and allows internal energy conversion to the excited triplet state (**Paper I** Figure 1). The resonant energy transfer from excited triplet state of the donor to the excited singlet energy state of fluorescent dye (acceptor) is kinetically delayed, resulting in a long lifetime of emission and amplification of emission intensity as the quantum yield (QY) of the donor is low compared to the QY of the acceptor. This physical phenomenon is researched and discussed in detail in further studies (Ligi *et al.* 2016).

5.1.2. Application of ARC-Lum probes in biochemical assay

The growing drug industry focusing on protein kinases and their inhibitors benefits from robust, reliable, and rapid assays for screening of large compound libraries. Sensitive binding and displacement assays based on ARC-Lum probes allow the usage of minute amounts of both, protein kinase and probe, excluding the need for antibodies or substrates and drastically reducing the time needed for analysis.

Several ARC-Lum probes have been synthesized for analysis of protein kinases (**Paper III**, Table 1). The application of probe ARC-1182 was further characterized in a displacement assay with PKAc and competitive inhibitors to provide additional information on planning optimal conditions of the experiment. The low-picomolar affinity (K_d = 20 pM) of ARC-1182:PKAc complex in combination with TR measurement of luminescence (TRL) intensity allows the determination of affinities of competitive inhibitors in a wide range. The possibility to employ ARC-Lum in high excess compared to the protein kinase without an increase in the non-specific signal enables the determination of 30-fold higher inhibitor affinities than that of the probe. The lowest resolvable affinity is determined by the solubility. Data analysis according to the classical Cheng-Prusoff equation (Cheng and Prusoff 1973) would result in values delineating from regression and is not applicable in the case of tight-binding inhibitors (**Paper III** Graph 5). Instead, the modified equation accounting the concentration of free inhibitor ($[I]_{50}$), not the total concentration of inhibitor (IC_{50}) should be used (Equation 5) (Nikolovska-Coleska *et al.* 2004). It was proposed that the limit of the resolvable range of affinities should be calculated at the point where $[I]_{50} = ½[E]_T$. In the presence of the highest concentration of probe ARC-1182 used (C = 80 nM) at 0.5 nM concentration of PKAc, the highest affinity of competitive inhibitor towards PKAc that can be determined is 60 fM (**Paper III** Graph 5 blue solid line). Decreasing the concentration of ARC-1182 to 0.5 nM, as low as 1 mM affinities of inhibitors are possible to resolve, which in practice can be limited by the insolubility of the inhibitors. Similar modeling of a resolvable range of affinities of a competitive inhibitor for specific probe:protein complex supports the selection of concentrations for acquiring a well-resolved and accurate displacement curve, as well as aiding the selection of the probe with an optimal affinity for a specific purpose.

Screening large libraries of compounds for finding a lead compound can be a highly time-consuming and costly process. The search for novel lead scaffolds usually begins with *in silico* mining from tens of thousands to millions of structures (Gong *et al.* 2016). Hundreds of compounds can be selected for biochemical characterization. Initial hit identification immensely speeds the process of finding potent lead compounds. This can be achieved by measuring the decrease percentage of the signal of the probe:target complex induced by a single concentration of competitive inhibitor (one-point analysis) and calculating the estimated IC_{50} by Equation 9. Estimation of IC_{50} from one-point

analysis correlates well with IC_{50} from the full displacement curve (**Paper III** Graph 8) in case the value of the measured point falls into the linear range of displacement. The linear range falls into the region $0.1IC_{50}<IC_x<10IC_{50}$, where IC_x corresponds to the concentration of inhibitor at which x % of TRL intensity is remained (Copeland 2013).

$$IC_{50} = \frac{IC_x}{\frac{100}{x} - 1}$$

Equation 9. IC_{50}, inhibitor concentration at the half-maximal signal; IC_x, inhibitor concentration at which x % of the signal is retained.

TRL-intensity assay based on the application of ARC-Lum probes serves as an efficient method for initial hit screening. Manual pipetting, incubation, and measurement of 384-well plate can highlight promising lead compounds within 1 hour. For comparison, SPR measurement for initial evaluation of 278 compounds needs 3 minutes per compound for a measurement cycle and a total of 14 hours for measurements, not including the time needed for the surface regeneration of the chip (Miura *et al.* 2016). The automated ARC-Lum-based assay is up-scalable to the 1536-well plate while retaining the short measurement time.

5.1.3. Application of ARC-Lum(Fluo) probes for cellular studies

The binding-responsive intramolecular TR-FRET property of ARC-Lum probes offers a unique possibility to monitor the activity of protein kinases in live cells and cell lysates without the need for labelling of proteins. The cell plasma membrane-penetrating property of hexa-arginine-comprising ARCs has been established, excluding the need for conjugation of the compound with additional transport vectors (Uri *et al.* 2002).

Genetically unmodified human embryonic kidney cells (HEK293) were incubated with the solution containing the ARC-Lum probe ARC-1139 (C = 10 μM). The intracellular localization of ARC-1139 was monitored with a fluorescence microscope: ARC-1139 quickly crossed cell plasma membrane, distributed into the cytoplasm and concentrated into special regions of nuclei, apparently nucleoli (**Paper I** Supplementary Figure 10).

Subsequently, C9H6 cells were supplemented with Forskolin in the presence of ARC-1139. FRSK activates AC and consequently, PKA. The released catalytic subunit PKAc of PKA interacts with the probe ARC-1139 leading to increase in long-lifetime luminescence intensity signal that was registered with PHERAstar luminescence platereader (Figure 3). An ATP-competitive inhibitor H89 was introduced after signal stabilization. H89 crosses cell plasma membrane and binds to PKAc with relatively high selectivity and affinity. H89 disrupted the complex between PKAc and ARC-1139, resulting in loss of long-

lifetime luminescence intensity. Furthermore, H89 reduced the luminescence intensity compared to its initial value. Thus ARC-Lum probes demonstrated the usability as intracellular sensors for monitoring real-time changes in the concentration of protein kinases in response to extracellular stimuli.

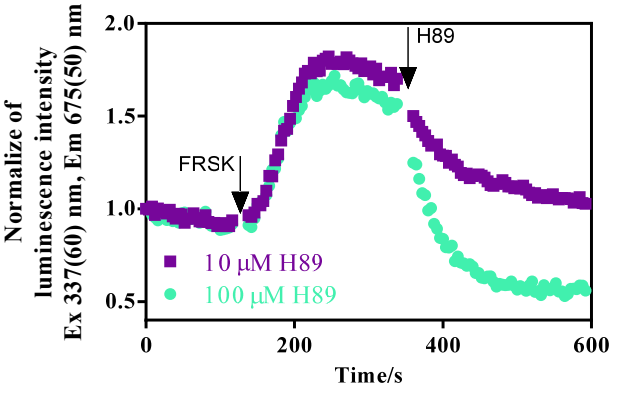

Figure 3. Real-time monitoring of PKA activity in living C9H6 cells after loading the cells with ARC-1139: time points of addition of Forskolin (FRSK, 25 μM) and 100 μM (green ●) or 10 μM (purple ■) H89 are marked with the arrows.

5.2. Structure-affinity and X-ray crystal structure studies of bifunctional inhibitors (Paper I, Paper II, unpublished results)

A new set of compounds was synthesized proceeding from results of crystal structure analysis of ARC-670:PKAc co-crystals (Pflug *et al.* 2010). Replacing the structure of ATP-competitive moiety of ARC-670 with 7-deazapurine led to the high affinity of the compounds, this property was subjected to further optimization. The potential of varying the length of α,ω-diacid linker was realized and the biochemical analysis of protein kinases PKAc, PKBγ, and ROCK2 showed that the optimal distance between the nucleoside-mimicking and peptide moieties was achieved by using α,ω-nonanedioic acid as the linker (**Paper II**, Table 1). This design led to the binder revealing the highest affinity towards PKAc to date, ARC-1411 that possesses one-digit picomolar K_d value ($K_{d,PKAc}$ = 3 ± 1 pM). At 1 μM concentration ARC-1411 inhibited many other basophilic protein kinases by more than 90% as tested in a commercial panel of protein kinases (**Paper II** Table S1).

The inhibitory potency (IC_{50}) of compounds in the phosphorylation reaction has been shown to correlate well with their affinity determined in a binding assay with FA (Vaasa *et al.* 2009) or TRL intensity readout (**Paper I** Figure 3A). Next, the thermal shift assay based on a comparison of the protein denaturation temperature with and without the presence of an inhibitor was conducted. ARC-type inhibitors strongly stabilized the structure of PKAc: compounds with low-

picomolar affinity shifted the denaturation temperature of PKAc from 42 °C to more than 58 °C (ΔT_m = 16 °C). K_d values obtained from TRL intensity based assay for 7-deazapurine-comprising ARCs correlated well with the ΔT_m values found from the thermal shift assay (Figure 4A, black data points, R = 0.97). ARC-inhibitors comprising different ATP-competitive moieties induced stronger thermal stabilization effect for inhibitors possessing equal or lower affinity (Figure 4A, blue data points). Therefore, the linear relationship between the logK_d and ΔT_m values holds better for inhibitors taking part in similar interactions or inducing similar conformational changes in the structure of the protein. The latter is evident from the crystal structure analysis of ARC-1411:PKAc co-crystal compared to that of ARC-1408 (PDB ID: 5IZF) or ARC-1416 (PDB ID: 5J5X) co-crystals. The –(D-Arg)$_6$–D-Lys–NH$_2$ peptide moiety attached to α,ω-nonanedioic acid in ARC-1411 sterically hinders the overall optimal positioning and interaction of the second Arg residue with the protein, directing it out towards the water environment and forcing the Gly-rich flap of PKAc into an open conformation (**Paper II** Figure 5B, Figure S7). In contrast, two Arg residues separated by the linker in ARC-1408 and Ala replacing α-Arg in the structure of ARC-1416 allow the adaption of the Gly-rich flap of PKAc the intermediate conformation (**Paper II** Figure 5B). The difference of open and intermediate conformations is the main reason why ARC-1416 stabilizes the structure of PKAc to a greater extent relative to its affinity compared to ARC-1415 (structure of ARC-1411 without terminal Lys) and ARC-1411 (Figure 4A). The measurements with PKBγ did not result in good linear correlation, as the PKBγ was not activated by phosphorylation at Thr 309, whereas the similar trend of increase in ΔT_m with an increase in affinity of respective ARC was evident (Figure 4B).

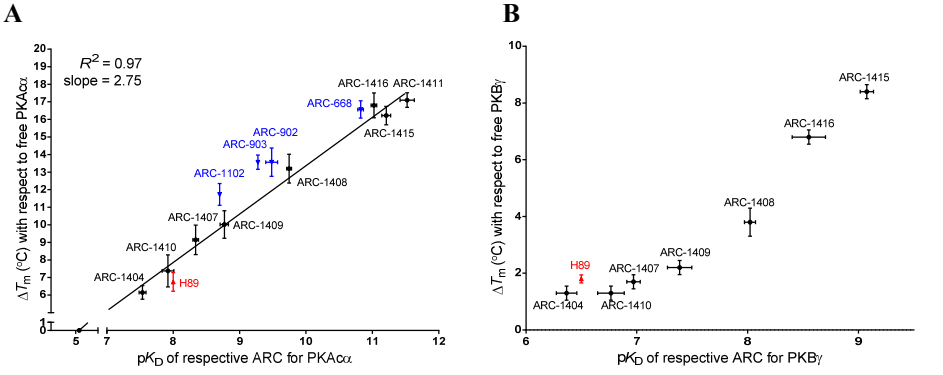

Figure 4. Correlation of thermal shift assay results (ΔT_m) with affinities (negative logarithm of K_d) measured with TRL-intensity assay for PKAc (n = 6) (A) and PKBγ (n = 3) (B). ARC-668, ARC-902, ARC-903, and ARC-1102 affinities found or calculated from literature (Lavogina *et al.* 2010b; Vaasa *et al.* 2009).

No PKB isoforms have been co-crystallized with ARCs and the exact positioning of the bifunctional inhibitor in the active site of PKBγ is unclear. Compared to PKAc, the thermal shift of PKBγ in the presence of ARC-1416 or ARC-1415 gave a better correlation with their measured affinities, suggesting that sequential D-Arg residue continuing from the linker are favored in terms of their placement. Further increase in affinity can, therefore, be achieved by replacing β-Arg in the structure of ARC-1411, possibly leading to sub-picomolar K_d values towards PKAc.

Isothermal titration calorimetry is continually a method of choice for gaining direct thermodynamic data (ΔG_B^0, ΔH_B^0, ΔS_B^0) regarding the binding between proteins or the protein and a ligand. These parameters were investigated for ARC-1404, ARC-1409, or ARC-1411 binding to PKAc (Figure 5). Binding of each ligand to PKAc possessed high value of ΔH_B^0, driven by polar interactions between the ligand and protein. The length of α,ω-nonanedioic acid linker within structures of ARC-1409 and ARC-1411 resulted in superior enthalpy term compared to ARC-1404 comprising α,ω-octanedioic acid linker. The insufficient length of the linker within ARC-1404 is possibly prohibiting the interaction between an Arg residue and Asp167 that is present in the crystal structure of ARC-1408, comprising an α,ω-nonanedioic acid linker. The term ΔS_B^0 was relatively large, especially for ARC-1409 and ARC-1411, resulting from tight fixation of the flexible structure of both ARC and PKAc upon association. Introducing a rigid structural fragment, for example by replacing β-Arg within ARC-1411 may reduce entropic gain from binding to PKAc and further improve the affinity. Despite useful thermodynamic data, ITC requires magnitudes higher concentration of reagents and is known to be inaccurate in determining high-affinity interactions by binding (Leavitt and Freire 2001).

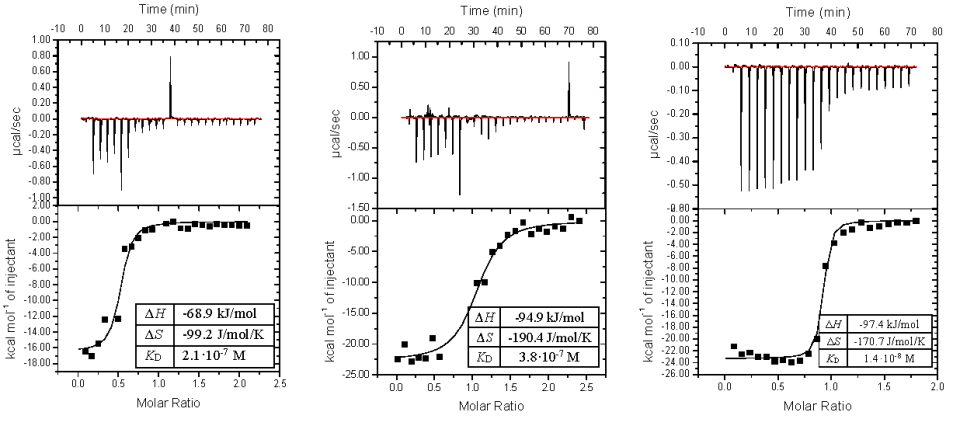

Figure 5. ITC binding isotherms for ARC-1404 (A), ARC-1409 (B), and ARC-1411 (C) with PKAc (n =1).

5.3. Bifunctional inhibitors as disruptors of PPIs (Paper II)

HTS of compound libraries, fragment-based drug design, and virtual screening are primarily limited to the detection of PPI inhibitors with affinities in the micromolar range (Nim *et al.* 2016), whereas inhibitors with higher affinity are required for successive disruption of tight-binding PPIs with K_D values below 200 nM. An inhibitor disrupting the PPI in a biochemical assay may fail in cells either due to insufficient cellular translocation of the inhibitor, degradation of the inhibitor in biological milieu, or due to the reinforcement of PPI in the complex cellular environment.

The concept of applying bifunctional inhibitors for disruption of strong PPIs was studied on PKA holoenzyme with ARC-type inhibitors. The subunits of PKA, PKAr and PKAc interact at protein substrate intraface of PKAc and are held together by the interaction with K_D value of 100 pM (Cheung *et al.* 2015). Disruption of this interaction directly by a reversible inhibitor at the protein substrate binding site needs a molecule with an impressive affinity that is unlikely to be achievable due to the nature of PPI intraface. Therefore, we employed ARCs that bind simultaneously to two substrate sites of PKAc – ATP-competitive moiety of the inhibitor enforces the interaction and protein substrate-competitive moiety disrupts the PPI between PKAc and PKAr.

First, ARC-1413, a 5-TAMRA-labelled probe ($K_{d,PKAc}$ = 5 pM) was used in FA-assay to detect the displacement by protein substrate competitive inhibitor PKArI or PKI (**Paper II** Figure 2). In comparison to the sub-nanomolar inhibitor ARC-902 ($K_{d,PKAc}$ = 0.33 nM) both PKArI and PKI displaced ARC-1413 with lower IC_{50} value. The addition of cAMP (50 μM) to the series containing PKArI resulted in the reformation of ARC-1413:PKAc complex (FA restored to the value of full complex), indicating that displacement was due to a specific interaction between PKArI and PKAc.

Next, a genetically engineered variant of PKA, cells expressing fusion proteins of PKA subunits with fluorescent proteins, was used as a cAMP sensor based on the measurement of the intensity of FRET between two fluorophores positioned in close proximity. The sensor was used to gain direct evidence that ARC-type high-affinity bifunctional ligands disrupt the interaction between regulatory and catalytic subunits of PKA. Lysate of C9H6 cells stably expressing the fusions of cyan fluorescent protein (CFP) and yellow fluorescent protein (YFP) with PKAr and PKAc (CHO cells stably expressing fusion proteins PKArIIβ-CFP and PKAcα-YFP), respectively, was separated and diluted 20-fold. The dilution series of ARC-1411 or ARC-902 disrupted the interaction of PKArIIβ-CFP:PKAc-YFP in the lysate, indicated by the decrease in FRET ratio (EX 427 nm, EM 530/480 nm) (**Paper II** Figure 3B). IC_{50} values for displacement of PKArIIβ from the PKA holoenzyme were 2 nM and 109 nM in the presence of ARC-1411 ($K_{D,PKAc}$ = 3 pM) and ARC-902 ($K_{D,PKAc}$ = 0,33 nM), respectively. In comparison, the disruption of PKA holoenzyme by cAMP resulted in an EC_{50} value of 48 nM, showing the high potency of ARC-1411 for disruption of the PKA holoenzyme.

It was not known whether H89 (Hidaka *et al.* 1990), a generic inhibitor of AGC-group protein kinases ($K_{D,PKAc}$ = 10 nM) (Viht *et al.* 2007) could bind into the ATP-pocket of PKAc in the tetrameric PKA holoenzyme. The effect of H89 on PKA holoenzyme was investigated using the lysate of C9H6 cells constituting fluorescent fusion proteins PKArIIβ-CFP and PKAcα-YFP. The titration series of H89 revealed that H89 did not disrupt PKA holoenzyme at concentrations up to 10 µM (Figure 6B). The PKA holoenzyme in 5% C9H6 cell lysate was disrupted by 1 µM ARC-902, resulting in cessation of FRET between fluorescent proteins and, consequently, disruption of the PKA tetramer (Figure 6B). In presence of 1 µM ARC-902, H89 displaced ARC-902 at higher concentrations and lead to recurrence of FRET, indicating reformation of the PKA holoenzyme (Figure 6A, Figure 6B). Interestingly, in the course of binding to the hydrophobic pocket of PKAc, H89 did not induce any detectable change in the conformation of the PKA holoenzyme according to FRET ratio (Figure 6C). However, only total disruption of the PKA holoenzyme can be excluded, as the distance between fused fluorescent proteins did not change and the conformational shifts within immediate proximity to the active site cannot be ruled out.

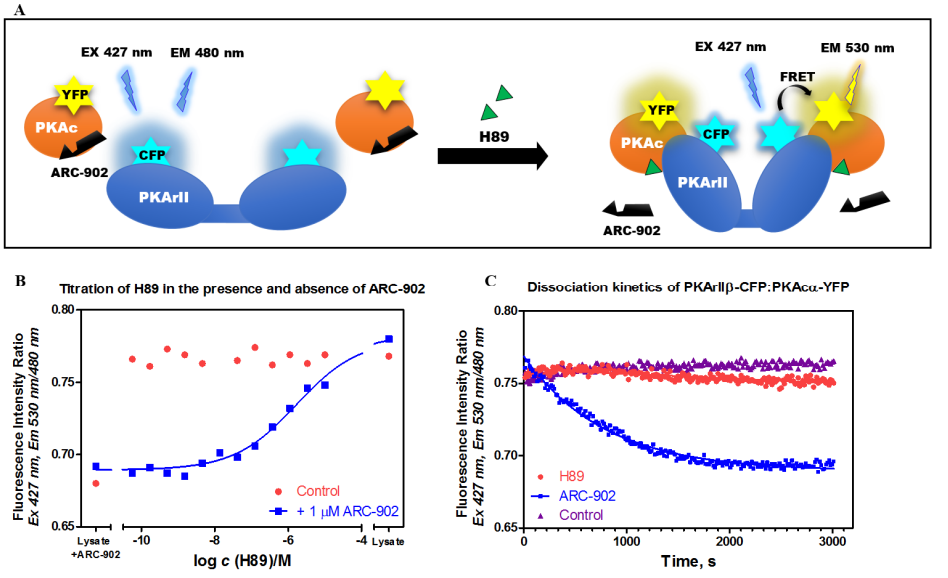

Figure 6. FRET assay for PKA holoenzyme dissociation. (A) Scheme of the proposed process of displacement of a PKArIIβ-competitive bisubstrate probe ARC-902 (black) from PKAcα (orange) by H89 (green), leading to PKA holoenzyme reformation and accompanying an increase in FRET from CFP to YFP. (B) Dilution series of H89 in the absence (red ●) and presence (blue ■) of 1 µM ARC-902. (C) Dissociation kinetic profiles of PKArIIβ-CFP:PKAcα-YFP with the addition of ARC-902 (10 µM, blue ■) or H89 (50 µM, red ●) at t = 0.

This result points to a fundamental difference between mono- and bifunctional ligands for inhibition of PKAc in intracellular milieu. H89, staurosporine, and other ATP-competitive inhibitors do not discriminate between PKAc-bound and free PKAc subunits, they can associate with PKAc in both states of the latter protein. Bifunctional inhibitors compete with PKAr for binding to PKAc, preferably interacting first with free subunits of PKAc to satisfy equilibrium conditions. At higher concentrations, bifunctional inhibitors disrupt the PKA holoenzyme and relocate PKAc away from the cell membranes where PKAr molecules are bound via interactions with AKAPs. Monofunctional inhibitors do not disrupt the PKA holoenzyme and the escape of monofunctional inhibitor-bound PKAc occurs only after binding of cAMP molecules to the PKAr dimer of the PKA holoenzyme. Considering that numerous AKAPs scaffold both AC and PKA (Dessauer 2009) proteins, the application of ARCs emerges as a novel tool for studying the underlying mechanism of this important signaling pathway.

The successful application of ARCs for disruption of the PKA holoenzyme led to the conception of employing bifunctional ligands for disruption of strong PPIs. According to this approach, one of the moieties of the bifunctional ligand competes with the partner protein for the interactions in the "hot spot" interface area of a protein, while the other moiety reinforces the interaction by occupying a well-defined binding site (*i.e.* the hydrophobic pocket). A key factor for achieving optimal binding of a bifunctional ligand to the target protein is the length of linker fragment. In the current work, this was achieved by utilizing an α,ω-diacid linker, which allowed the atom-wise fine-tuning of the distance between two moieties, improving the affinity 17-fold towards PKAc, 10-fold towards PKBγ, and 5-fold towards ROCKII (**Paper II** Table 1, ARC-1409 compared to ARC-1404). The approach of using a bifunctional ligand and employing an "affinity hook" is limited to proteins adjoined by a hydrophobic pocket that are participating in PPIs, possibly covering the whole purinome composed of 3200 protein members (Ambrosi 2009). Bifunctional inhibitors ensure the disruption of targeted PPI at lower concentrations due to their high affinity (*i.e.* ARC-1411). The introduction of such disruptors of PPIs into drug development pipelines presumes to bypass the limits of "*the Lipinski's Rule of Five*".

5.4. Dissociation kinetics assays utilizing ARC-Lum probes (Paper I, Paper IV, unpublished results)

5.4.1. Measurement of dissociation kinetics of ligand: protein complex using TRL-based assay

Information regarding the dissociation rate of a molecular complex is important for the construction of a potent inhibitor possessing long residence time. Without addressing dissociation kinetics of the ligand:protein complex, highly potent lead compounds may be discarded in assays based on the data of K_D

alone. The main reason for not characterizing dissociation kinetics of a molecular complex is frequently the limited number of assays that provide reliable data in conjunction with a simple setup of the assay.

The capability of TRL intensity assay was studied for characterization of dissociation kinetics of complexes of PKAc with different ligands (Figure 7). This setup is based on mixing a ligand under observation with the target protein kinase to achieve the level of >90% bound kinase. Thereafter, ARC-Lum probe is added in excess (at 50–300 nM concentration, depending on the affinity of the competitive ligand) to achieve complete displacement of the inhibitor under study and the TRL intensity is monitored in time. A similar setup utilizing the FA readout instead of TRL intensity can only be used in conditions where the fraction of free fluorescence probe after displacing the inhibitor is small. The association rate of ARC-type bifunctional ligands with PKAc has been shown to be diffusion limited (Viht *et al.* 2007) and the resulting time-dependent increase in TRL-intensity characterizes the dissociation rate of ligand in complex with PKAc. The found residence time of ARC-583 on PKAc (Table 1) was well comparable to the time established previously with an SPR measurement (Figure 7A) (Viht *et al.* 2007). Limited by the equipment (PHERAstar Plus) and manual pipetting, the highest measurable k_{off} for the ligand:PKAc complex was 0.15 s^{-1}, corresponding to the residence time of more than 6 s. Therefore, due to their short residence time on PKAc, this assay failed to characterize most of the tested ATP-competitive inhibitors except staurosporine, for which TRL signal resulted in a resolvable dissociation profile (τ = 20 s). The assay based on TRL intensity can be utilized for measuring faster dissociation kinetics by reducing the time between mixing and initiation of luminescence intensity measurements with the help of a quick dispensing/mixing system (PheraSTAR FL with automated injectors) or by the application of a flow equipment.

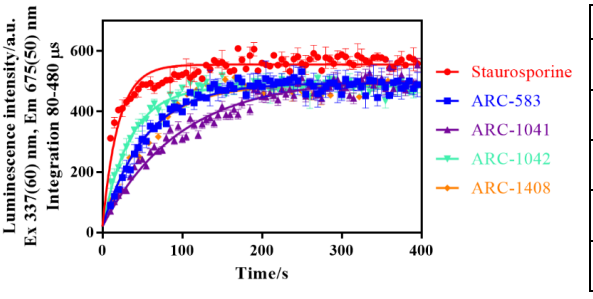

Ligand	k_{off}/s^{-1} (SEM)	τ/s
staurosporine	$5.0 \cdot 10^{-2}$ ($2.5 \cdot 10^{-3}$)	20.0
ARC-583	$1.8 \cdot 10^{-2}$ ($0.7 \cdot 10^{-3}$)	54.7
ARC-1041	$1.0 \cdot 10^{-2}$ ($0.3 \cdot 10^{-3}$)	96.6
ARC-1042	$2.8 \cdot 10^{-2}$ ($0.9 \cdot 10^{-3}$)	35.2
ARC-1408	$1.9 \cdot 10^{-2}$ ($1.0 \cdot 10^{-3}$)	53.8

Figure 7. Measurement of ARC-1063(100 nM):PKAc(1 nM) binding by a time-dependent increase in TRL-intensity, limited by k_{off} of respective inhibitor. A) Kinetic profile for dissociation of staurosporine (red ●), ARC-583 (blue ■), ARC-1041 (purple ▲), ARC-1042 (green ▼), or ARC-1408 (orange ♦) from the complex with PKAc (n = 2). B) Dissociation rate constants (SEM, standard error of the mean) and mean residence times (τ) found for the respective ligands on PKAc.

The described assay based on TRL intensity measurement offers a rapid homogeneous method for characterization of binding kinetics of the compounds. Furthermore, combining the method with automated pipetting in TR-capable microplate readers and one-point analysis (described in 4.1.2.), multiple essential parameters characterizing the thermodynamics and kinetics of association of a ligand with the target protein can be extracted simultaneously.

5.4.2. Facilitation of dissociation rate of bifunctional inhibitor from complex with protein kinase

Dissociation process of the complex between a ligand and a protein may consist of several steps (Vauquelin and Van Liefde 2012). Separation of microscopic steps of the process is experimentally difficult and is rarely achieved, macroscopic steps involve an overall change in the 3-D structure of the protein (induced fit) and subsequent escape of the ligand from the protein. In a simple case, the contribution of conformational change in protein to the overall rate of dissociation is minute and can be classified as a microscopic event. Regardless of the exact mechanism, dissociation of the complex follows the kinetics of the first order reaction and the kinetics is independent of the concentration of the complex (Pollard 2010).

The application of ARC-Lum(Fluo) probes for intracellular studies resulted in an unexpected kinetic behavior of the probes. The addition of the competitive inhibitor H89 induced a faster dissociation of ARC-1139 and PKAc in C9H6 cells than anticipated, as revealed by the decrease in TRL intensity (Figure 3). Subsequent biochemical experiments showed inconsistent k_{off} values for the complexes of bifunctional probes and protein kinases.

The effect of competitive inhibitors on the dissociation rate of molecular complexes was investigated on the example of the complex of ARC-1063 and PKAc (**Paper IV** Figure 1). All tested ligands (inhibitors and substrates) facilitated the rate of dissociation of ARC-1063:PKAc complex at higher concentrations (Figure 8). Thereby, both monofunctional and bifunctional inhibitors induced the effect of facilitation towards the rate of dissociation.

This finding suggested that bifunctional inhibitors possess two macroscopic dissociation steps. The results of accelerated dissociation suggested that the moiety of the bifunctional ligand directed to the ATP-binding pocket associates with and dissociates from the deep hydrophobic pocket with the rate (characterized by $k_{a,1}$ and $k_{d,1}$, respectively, Figure 9A) similar to that of the monofunctional ligand (structurally corresponding to the dissociated moiety). The relatively small dissociation rate constants ($k_{off} < 0.01\ s^{-1}$) that are characteristic for tight-binding bifunctional molecules (ARC-type inhibitors) result from the favorable re-binding of the ATP-competitive moiety due to the existence of the second moiety. The second moiety is continuously bound to the protein and holds the detached moiety in close proximity to its binding site.

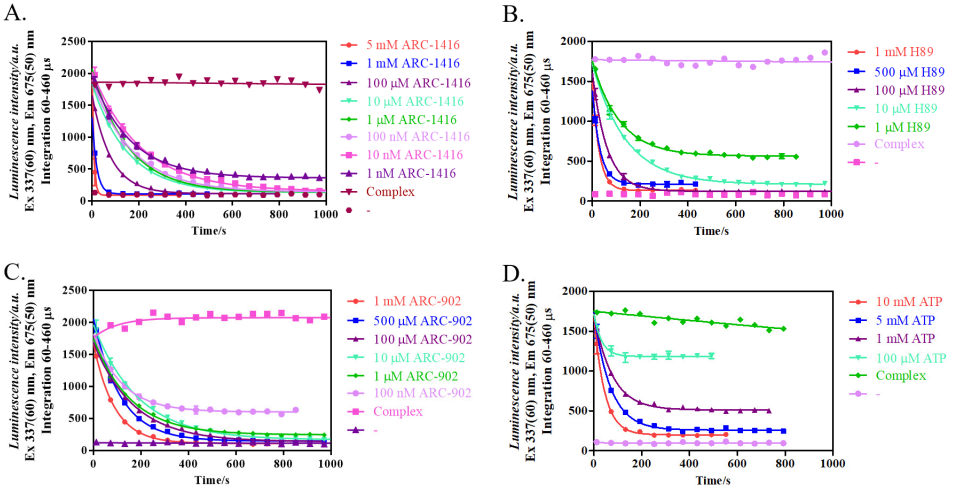

Figure 8. Dissociation profile of ARC-1063:PKAc complex initiated by addition of the following ligands at t = 0 s. A) Bifunctional inhibitor ARC-1416, concentration range 1 nM – 5 mM. B) ATP-competitive inhibitor H89, concentration range 1 µM – 1 mM. C) Bifunctional inhibitor ARC-902, concentration range 100 nM – 1 mM. D) ATP (in the presence of 10 mM Mg^{2+}), concentration range 100 µM – 10 mM. Complex, ARC-1063:PKAc w/o competitive inhibitor; Dash (-),1 nM ARC-1063.

The large excess concentration of the competitive compound increases the probability that the latter molecules occupies the ATP-binding site of the protein kinase within the dissociation-association event of an ATP-competitive fragment of the bifunctional ligand. The competitive compound (for example, ATP) can dissociate quickly, however its high concentration allows another molecule to occupy the binding pocket instead of ATP-competitive moiety of bifunctional ligand. The re-binding of ATP-competitive moiety of the bifunctional ligand is prohibited and subsequent dissociation of the peptide moiety is accelerated, leading to facilitated full escape of the bifunctional ligand. Herein, the facilitated dissociation rate constant ($k_{\mathrm{off,fac}}$) for the complex between a bifunctional ligand and target protein characterizes the rate at an infinite concentration of the competitive ligand. For a bifunctional ligand, under completely facilitated conditions this leads to dissociation rate constants according to the equation $k_{\mathrm{off,fac}} = \frac{k_{\mathrm{d,1}} \cdot k_{\mathrm{d,2}}}{k_{\mathrm{d,1}} + k_{\mathrm{d,2}}}$ or $k_{\mathrm{off,fac}} = \frac{k_{\mathrm{d,3}} \cdot k_{\mathrm{d,3}}}{k_{\mathrm{d,3}} + k_{\mathrm{d,3}}}$, depending on the nature of both bifunctional ligand and competitive ligand. In case the competitive ligands were applied at concentrations less than 1 µM, the dissociation of ARC-1063:PKAc complex showed a plateau of residence time values (**Paper IV** Figure 1D). The upper plateau value of residence time (202 s for ARC-1063 on PKAc) designates the intrinsic residence time of the bifunctional ligand on protein. The intrinsic residence time (τ_{int}) and intrinsic

dissociation rate constant ($k_{off,int}$) characterize the dissociation rate of a complex in the absence of a competitive ligand (Figure 9B). Despite that rates of individual macroscopic dissociation steps ($k_{d,1}$, $k_{d,2}$, $k_{d,3}$, $k_{d,4}$) may be relatively large (> 0.1 s^{-1}), the re-binding of the dissociated moiety is favored due to spatial proximity to the binding site (Vauquelin and Van Liefde 2012), leading to formation of full complex by following rate constant $k_{a,1}$ or $k_{a,3}$. Intrinsic residence time of a bifunctional ligand on protein can be described by rate constant $k_{\mathrm{off,int}} = \frac{k_{d,1} \cdot k_{d,2}}{k_{d,1}+k_{a,1}+ k_{d,2}}$ or $k_{\mathrm{off,int}} = \frac{k_{d,3} \cdot k_{d,4}}{k_{d,3}+k_{a,3}+ k_{d,4}}$ (Tummino and Copeland 2008).

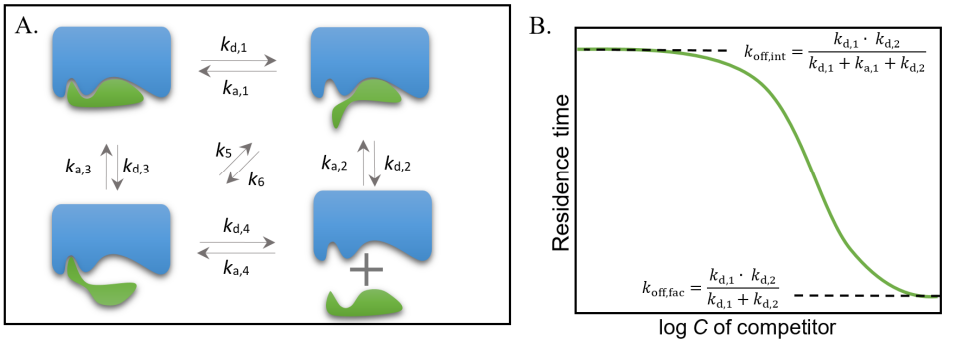

Figure 9. Facilitated dissociation of the complex of a bifunctional ligand and protein. A) Dissociation of the complex between a bifunctional ligand and protein kinase. B) The difference between the values of the residence time of higher and lower plateaus reveals the total contribution of the fast re-binding event of the detached moiety. $k_{off,int}$, the intrinsic residence time of complex between bifunctional ligand and protein; $k_{off,fac}$, the facilitated residence time of complex.

The facilitation of dissociation rate was evident from 1 µM to over 10 µM concentration of displacing compound and revealed the dependence on the structure of ATP-competitive moiety (**Paper IV** Figure 1B, Figure 1D). ARC-1416 [comprising 4-(piperazin-1-yl)-7H-pyrrolo[2,3-d]pyrimidine] and H89 {N-[2-(*p*-bromocinnamylamino)ethyl]-5-isoquinolinesulfonamide} facilitated the dissociation of ARC-1063:PKAc at lower concentrations compared to ATP and ARC-902 (comprising adenosine). This difference from the structure of competitive inhibitor arises from their association rates with PKAc, wherein slower associating compounds require a higher concentration to increase the probability of occupying vacated ATP-binding site by bifunctional ligand.

Two molecular interaction mechanisms were found that could explain the phenomenon of facilitated dissociation. First, the effect is similar to the proposed model of rapid re-binding, in which the dissociation of two molecules is followed by fast association, as the molecules continue to reside within close proximity (Paramanathan *et al.* 2014). In the presence of high concentration of competitive ligand, the re-binding event is prevented in a concentration-dependent manner due to the occupation of the site by the competing ligand.

Second, the dissimilar facilitated rates by different structures (**Paper IV** Figure 1D) of competitive ligands indicate the formation of the ternary complex (Figure 10), as the association rates of competitors have a significant effect, contrary to the model of rapid rebinding, and the discovered effect of facilitation was several folds stronger. The formation of ternary complex lowers the activation energy needed for the full escape of bifunctional ligand and subsequent binding of the competitive ligand.

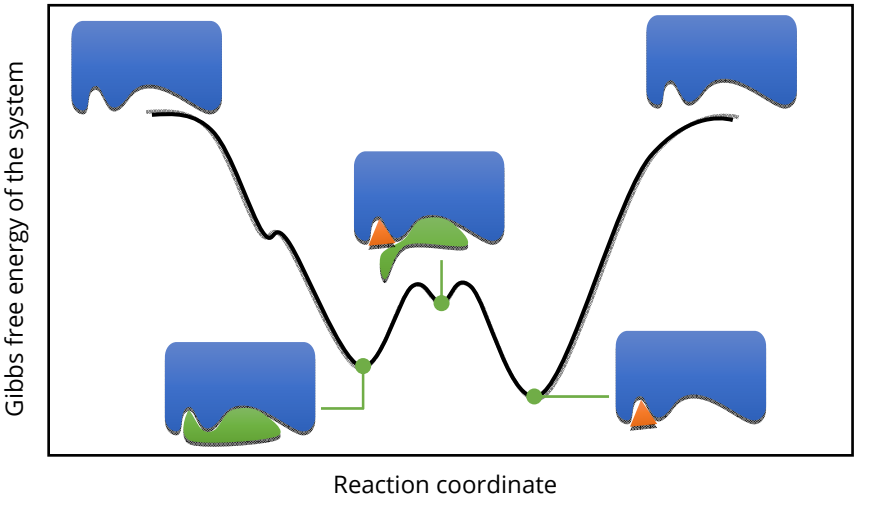

Figure 10. Reaction path for a possible mechanism of dissociation rate facilitation by the competitive inhibitor from protein kinase (blue structure). The lower energy for the complex with monofunctional inhibitor (orange triangle) indicates the conditions of the system where the concentration of the latter greatly exceeds a concentration of the bifunctional ligand (green structure).

The proposed description of the facilitated dissociation is in accord with the acknowledged model of avidity or "forced proximity" of bifunctional ligands, mostly discussed in case of antibodies (Vauquelin and Van Liefde 2012). A brief description of facilitated dissociation phenomenon has been given for complex between a homobifunctional inhibitor and a dimer of synthetic carbonic anhydrase II [$(CAII)_2$] (Mack *et al.* 2012). Herein, competitive inhibitor facilitated the dissociation of a bimolecular complex, in which the hetero-bifunctional ligand binds into two distinct binding sites separated by a short distance of 1.5 nm within a single protein.

6. CONCLUSIONS

The current thesis is focused on the characterization and application of bifunctional ligands, adenosine analogue and oligo-arginine conjugates (ARCs), for studying protein kinases in biochemical assays and intracellular format. The literature overview briefly introduces the basics of proteins, the importance of protein-protein interactions (PPIs) in living cells, inhibitors of protein kinases and PPIs, and methods involved in protein studies. These topics are relevant in regard to the main results of this thesis, which are summarized as follows:

- ARC-Lum probes were discovered which exhibit protein binding-induced long-lifetime photoluminescence property. The rationale for employing such probes in biochemical assays and cellular applications was discussed.
- The assay based on time-resolved measurement of luminescence (TRL) intensity using ARC-Lum probes was validated for the screening of protein kinase inhibitors possessing affinities in a wide range.
- Structure-affinity studies supported by the TRL assay, thermal shift assay, and isothermal titration calorimetry combined with the information obtained from X-ray analysis of co-crystal structures led to the development of novel ARC-type bifunctional ligands possessing one-digit picomolar affinity towards PKAc. Novel series of ARCs was characterized in TRL assay towards protein kinases PKAc, PKBγ, and ROCKII.
- Based on successful disruption by ARCs of a stable protein complex (PKA holoenzyme) possessing K_D value of 100 pM formed between PKA subunits PKAr and PKAc. An approach was proposed for targeting strong PPIs with bifunctional inhibitors possessing a PPI-competitive moiety along with "affinity hook" that occupies an adjacent and well-defined binding site.
- TRL assay for the measurement of dissociation kinetics of a complex between a protein kinase and inhibitor was developed and characterized.
- Facilitated dissociation kinetics of a complex between a bifunctional ligand and protein kinase was discovered. This property was further characterized and possible explanations for the phenomenon were discussed.

7. SUMMARY IN ESTONIAN

Bifunktsionaalsed inhibiitorid ja fotoluminestsents-sondid valgukomplekside uurimiseks

Raku elutegevust reguleerivad signaalirajad moodustavad keerulise süsteemi, milles omavad keskset rolli proteiinkinaasid. Proteiinkinaasid katalüüsivad fosforüülrühma ülekannet nukleotiidilt sihtvalgule, mõjutades seeläbi sihtvalgu funktsioone nagu lokalisatsioon ja aktiivsus. Kõrvalekalded normaalsest proteiinkinaasi aktiivsusest, mis on valdavalt põhjustatud geenimutatsioonidest või häiretest ekspressioonis, võivad põhjustada raskesti ravitavaid haigusi nagu neurodegeneratiivsed (Parkinson, Alzheimer) ja südame-veresoonkonna haigused, diabeet ning vähkkasvajad (Tönges *et al.* 2012; Cho *et al.* 2001; Morgan-Fisher *et al.* 2013). Proteiinkinaaside aktiivsuse reguleerimine väikese molekulmassiga inhibiitoritega on seetõttu ravimiarenduse pingsa tähelepanu all ning 28 proteiinkinaaside inhibiitorit on kasutusel vähiravimina (Wu *et al.* 2016). Ravimikandidaatide arendustöö toetamiseks on vajalikud efektiivsed biokeemilised meetodid, mis võimaldavad potentsiaalsete inhibiitorite kiiret tuvastamist ja nende toimemehhanismide iseloomustamist.

Käesoleva töö tulemusena töötati välja ja iseloomustati uudne meetod biokeemilisteks katseteks, mis põhineb orgaanilise madalmolekulaarse sondi (ARC-Lum-sondi) aeglase kustumisega luminestsentsi eluea mõõtmisel. Tartu Ülikooli keemia instituudis välja arendatud ARC-Lum-sondid on bifunktsionaalsed proteiinkinaaside inhibiitorid, mis koosnevad ATP sidumistaskusse seonduvast tiofeeni või selenofeeni fragmenti sisaldavast osast, valk-substraadiga konkureerivast peptiidsest fragmendist ja neid ühendavast linkerist. Ergastamisel lähis-UV kiirgusega avastati sisemolekulaarne Förster-tüüpi resonantse energia ülekande (FRET) mehhanism tiofeeni või selenofeeni fragmendilt (FRET-doonor) peptiidse fragmendi külge konjugeeritud fluorivärvile (FRET-aktseptor) [ARC-Lum(Fluo)]. Seostumata ARC-Lum(Fluo) luminestsents sumbus kiiresti (< 10 ns), proteiinkinaasiga kompleksis pikenes luminestsentsi eluiga 20–270 mikrosekundini, sõltuvalt proteiinkinaasist. Valgu sidumisest sõltuv luminestsentsi pikk eluiga võimaldab ARC-Lum(Fluo)-sonde kasutada aegviivitusega mõõterežiimis, vähendades märgatavalt mittespetsiifiliste signaalide mõjusid. Vastav omadus võimaldas iseloomustada mitme basofiilse proteiinkinaasi aktiivsust biokeemilises analüüsimeetodis, inhibiitorite sidumise efektiivsust laias afiinsuste vahemikus, proteiinkinaas:inhibiitor-kompleksi dissotsiatsioonikineetikat ja jälgida reaalajas proteiinkinaasi aktiivsust imetajarakkudes.

Mahukate struktuur-aktiivsus uuringute ja ARC:PKAc kooskristallide röntgenstruktuur-analüüsi tulemustest lähtudes arendati uudse struktuuriga bifunktsionaalsed ARC-tüüpi inhibiitorid, mis saavutasid senikirjeldatud inhibiitoritest kõrgema afiinsuse proteiinkinaasi PKAc suhtes (K_d < 10 pM). Nende inhibiitorite puhul näidati linkeri pikkuse mõju olulisust afiinsusele ning juurutati sünteesiskeem kahe funktsionaalse osa vahelise kauguse varieerimiseks.

Pikomolaarse afiinsusega fluorestsents-sondi ARC-1413 kasutati PKA holoensüümi alaühikute (PKAc ja PKAr) vahelise valk-valk interaktsiooni afiinsuse määramiseks fluorestsentsanisotroopia meetodil. Saadud tulemus näitas, et bifunktsionaalseid inhibiitoreid on võimalik kasutada terapeutiliselt oluliste, kuid monofunktsionaalsete inhibiitorite jaoks liigselt kõrge afiinsusega valkudevaheliste interaktsioonide lõhkumiseks. Inhibiitorite toimemehhanismi edasiseks uurimiseks valmistati lüsaat rakkudest, mis sisaldas geneetiliselt muundatud PKA alaühikuid: kollase fluorivalguga PKAc liitvalku (PKAcα-YFP) ja rohelise fluorivalguga PKAr liitvalku (PKArIIβ-GFP). Bifunktsionaalne inhibiitor ARC-1411 lõhkus kontsentratsioonist sõltuvalt PKAcα-YFP2:PKArIIβ-GFP2 tetrameerse holoensüümi, mis tuvastati luminestsentsi intensiivsuste suhte muutumise järgi YFP ja GFP kanalites. PKA alaühikute vahelise PPI lõhkumine pikomolaarse afiinsusega (K_D = 3 pM) bifunktsionaalse inhibiitoriga ARC-1411 toimus üle 20 korra madalamal kontsentratsioonil, kui füsioloogilise PKA holoensüümi aktivaatori, sekundaarse virgatsaine cAMP-ga. Erinevalt monofunktsionaalsest inhibiitorist H89, mis seondus samuti PKA holoensüümiga, omab raku plasmamembraani läbiv ARC-inhibiitor võimet eristada vaba ja seostunud PKAc alaühikut ning soodustab PKAc transporti rakumembraanidest eemale.

ARC-sondide abil proteiinkinaaside aktiivsuse jälgimisel rakkudes ja ARC-inhibiitorite dissotsiatsioonikineetika uurimiste käigus avastati bifunktsionaalsete inhibiitorite hõlbustatud dissotsiatsiooni nähtus. Konkureerivad inhibiitorid kiirendavad bifunktsionaalse inhibiitori ja proteiinkinaasi vahelise kompleksi dissotsiatsiooni. Bifunktsionaalse inhibiitori üks aktiivosa dissotsieerub võrdlemisi kiiresti, kuid kompleksi täielik dissotsiatsioon on takistatud sünergistiliselt teise fragmendi kaudu, mis jääb valguga seotuks. Dissotsieerunud funktsionaalse osa assotsiatsioon sidumistaskuga on soodustatud ruumilise läheduse tõttu ja sellest tuleneb kompleksi aeglane lagunemine. Konkurentse inhibiitori lisamine suures ülehulgas suurendab tõenäosust, et bifunktsionaalse inhibiitori osalise dissotsiatsiooni ajal hõivab konkurentne inhibiitor vabanenud sidumistasku, soodustades bifunktsionaalse inhibiitori täielikku dissotsiatsiooni. Avastatud nähtus näitab kompleksi kineetiliste parameetrite iseloomustamise olulisust, kuna hõlbustatud dissotsiatsioon ilmneb mõnede ligandide (näit. ATP) füsioloogiliselt saavutatavate kontsentratsioonide juures.

Uurimistöös kasutati ARC-tüüpi bifunktsionaalseid inhibiitoreid ja fotoluminestsents-sonde mitmekülgseks proteiinkinaaside ja nende inhibiitorite iseloomustamiseks. Kirjeldatud bifunktsionaalsete ühendite edukus tugevate valk-valk interaktsioonide lõhkumisel lisab uudse võimaluse valkude kompleksseerumise mõjutamiseks ravieesmärgil.

REFERENCES

Abeykoon J. P., Yanamandra U., Kapoor P. (2017) New developments in the management of Waldenström macroglobulinemia. *Cancer Manag. Res.* **9**, 73–83.

Agafonov R. V., Wilson C., Otten R., Buosi V., Kern D. (2014) Energetic dissection of Gleevec's selectivity toward human tyrosine kinases. *Nat. Struct. Mol. Biol.* **21**, 848–853.

Agarwal A., MacKenzie R. J., Pippa R., Eide C. A., Oddo J., Tyner J. W., Sears R., et al. (2014) Antagonism of SET using OP449 enhances the efficacy of tyrosine kinase inhibitors and overcome drug resistance in myeloid leukemia. *Clin Cancer Res.* **15**, 2092–2103.

Alessi D. R., Andjelkovic M., Caudwell B., Cron P., Morrice N., Cohen P., Hemmings B. A. (1996) Mechanism of activation of protein kinase B by insulin and IGF-1. *EMBO J.* **15**, 6541–51.

Ambrosi N. D. (2009) Membrane compartments and purinergic signalling: the purinome, a complex interplay among ligands, degrading enzymes, receptors and transporters. *FEBS J.* **276**, 318–329.

Anfinsen C. B. (1973) Principles that govern the folding of protein chains. *Science (80–.).* **181**, 223–230.

Arai M., Iwakura M., Matthews C. R., Bilsel O. (2011) Microsecond subdomain folding in dihydrofolate reductase. *J. Mol. Biol.* **410**, 329–342.

Arencibia J. M., Pastor-Flores D., Bauer A. F., Schulze J. O., Biondi R. M. (2013) AGC protein kinases: From structural mechanism of regulation to allosteric drug development for the treatment of human diseases. *Biochim. Biophys. Acta – Proteins Proteomics* **1834**, 1302–1321.

Arkin M. R., Tang Y., Wells J. A. (2014) Small-Molecule Inhibitors of Protein-Protein Interactions: Progressing toward the Reality. *Chem. Biol.* **21**, 1102–1114.

Ataullakhanov F. I., Vitvitsky V. M. (2002) What Determines the Intracellular ATP Concentration. *Biosci. Rep.* **22**, 501–511.

Bach A., Clausen B. H., Moller M., Vestergaard B., Chi C. N., Round A., Sorensen P. L., et al. (2012) A high-affinity, dimeric inhibitor of PSD-95 bivalently interacts with PDZ1-2 and protects against ischemic brain damage. *Proc. Natl. Acad. Sci.* **109**, 3317–3322.

Baker M. S., Ahn S. B., Mohamedali A., Islam M. T., Cantor D., Verhaert P. D., Fanayan S., et al. (2017) Accelerating the search for the missing proteins in the human proteome. *Nat. Commun.* **8**, 14271.

Bazin H., Préaudat M., Trinquet E., Mathis G. (2001) Homogeneous time resolved fluorescence resonance energy transfer using rare earth cryptates as a tool for probing molecular interactions in biology. *Spectrochim. acta Part A, Mol. Biomol. Spectrosc.* **57**, 2197–2211.

Beltrao P., Bork P., Krogan N. J., Noort V. Van (2013) Evolution and functional cross-talk of protein post-translational modifications. *Mol. Syst. Biol.* **9**, 1–13.

Bogoyevitch M. A., Barr R. K., Ketterman A. J. (2005) Peptide inhibitors of protein kinases-discovery, characterisation and use. *Biochim. Biophys. Acta* **1754**, 79–99.

Bononi A., Agnoletto C., Marchi E. De, Marchi S., Patergnani S., Bonora M., Giorgi C., et al. (2011) Protein kinases and phosphatases in the control of cell fate. *Enzyme Res.* **2011**, 329098.

Brazil D. P., Hemmings B. A. (2001) Ten years of protein kinase B signalling: A hard Akt to follow. *Trends Biochem. Sci.* **26**, 657–664.

Brazil D. P., Park J., Hemmings B. A. (2002) PKB binding proteins: Getting in on the Akt. *Cell* **111**, 293–303.

Buchner G. S., Murphy R. D., Buchete N. V., Kubelka J. (2011) Dynamics of protein folding: Probing the kinetic network of folding-unfolding transitions with experiment and theory. *Biochim. Biophys. Acta – Proteins Proteomics* **1814**, 1001–1020.

Camacho-Carvajal M. M., Wollscheid B., Aebersold R., Viktor S., Schamel W. W. (2004) Two-dimensional Blue Native/SDS Gel Electrophoresis of Multi-Protein Complexes from Whole Cellular Lysates. *Mol. Cell. Proteomics* **3**, 176–182.

Chatr-Aryamontri A., Breitkreutz B. J., Oughtred R., Boucher L., Heinicke S., Chen D., Stark C., et al. (2015) The BioGRID interaction database: 2015 update. *Nucleic Acids Res.* **43**, D470–D478.

Chen J., Sawyer N., Regan L. (2013) Protein-protein interactions: General trends in the relationship between binding affinity and interfacial buried surface area. *Protein Sci.* **22**, 510–515.

Chen X., Dai J. C., Orellana S. A., Greenfield E. M. (2005) Endogenous protein kinase inhibitor Y terminates immediate-early gene expression induced by cAMP-dependent protein kinase (PKA) signaling: Termination depends on PKA inactivation rather than PKA export from the nucleus. *J. Biol. Chem.* **280**, 2700–2707.

Cheng Y., Prusoff W. H. (1973) Relationship between the inhibition constant (K1) and the concentration of inhibitor which causes 50 per cent inhibition (I50) of an enzymatic reaction. *Biochem. Pharmacol.* **22**, 3099–3108.

Cheung J., Ginter C., Cassidy M., Franklin M. C., Rudolph M. J., Robine N., Darnell R. B., Hendrickson W. A. (2015) Structural insights into mis-regulation of protein kinase A in human tumors. *Proc. Natl. Acad. Sci.* **112**, 1374–1379.

Cho H., Mu J., Kim J. K., Thorvaldsen J. L., Chu Q., Crenshaw E. B., Kaestner K. H., Bartolomei M. S., Shulman G. I., Birnbaum M. J. (2001) Insulin resistance and a diabetes mellitus-like syndrome in mice lacking the protein kinase Akt2 (PKB beta). *Science* **292**, 1728–1731.

Clackson T., Wells J. A. (1995) A hot spot of binding energy in a hormone-receptor interface. *Science (80–.).* **267**, 383–386.

Copeland R. A. (2013) Lead Optimization and Structure-Activity Relationships for Reversible Inhibitors, in *Eval. Enzym. Inhib. Drug Discov.*, pp. 169–201. John Wiley & Sons, Inc., Hoboken, NJ, USA.

Copeland R. A., Pompliano D. L., Meek T. D. (2006) Drug-target residence time and its implications for lead optimization. *Nat. Rev. Drug Discov.* **5**, 730–739.

Corson T. W., Aberle N., Crews C. M. (2008) Design and applications of bifunctional small molecules: Why two heads are better than one. *ACS Chem. Biol.* **3**, 677–692.

Dames S. A., Martinez-Yamout M., Guzman R. N. De, Dyson H. J., Wright P. E. (2002) Structural basis for HIF-1 alpha/CBP recognition in the cellular hypoxic response. *Proc. Natl. Acad. Sci. U. S. A.* **99**, 5271–5276.

Datta S. R., Dudek H., Xu T., Masters S., Haian F., Gotoh Y., Greenberg M. E. (1997) Akt phosphorylation of BAD couples survival signals to the cell-intrinsic death machinery. *Cell* **91**, 231–241.

Dessauer C. W. (2009) Adenylyl cyclase-A-kinase anchoring protein complexes: the next dimension in cAMP signaling. *Mol. Pharmacol.* **76**, 935–941.

Du X., Li Y., Xia Y.-L., Ai S.-M., Liang J., Sang P., Ji X.-L., Liu S.-Q. (2016) Insights into protein–ligand interactions: mechanisms, models, and methods. *Int. J. Mol. Sci.* **17**, 144.

Dyson H. J., Wright P. E. (2005) Intrinsically unstructured proteins and their functions. *Nat. Rev. Mol. Cell Biol.* **6**, 197–208.

Engh R. a., Girod A., Kinzel V., Huber R., Bossemeyer D. (1996) Crystal structures of catalytic subunit of cAMP-dependent protein kinase in complex with isoquinolinesulfonyl protein kinase inhibitors H7, H8, and H89. *J. Biol. Chem.* **271**, 26157–26164.

Farmer T. B., Caprioli R. M. (1998) Determination of protein-protein interactions by matrix-assisted laser desorption/ionization mass spectrometry. *J. Mass Spectrom.* **33**, 697–704.

Fields S., Song O. (1989) A novel genetic system to detect protein-protein interactions. *Nature* **340**, 245–246.

Finkelstein A. V., Badretdin A. J., Galzitskaya O. V., Ivankov D. N., Bogatyreva N. S., Garbuzynskiy S. O. (2017) There and back again: Two views on the protein folding puzzle. *Phys. Life Rev.* **1**, 1–16.

Glickman J. F. (2012) Assay development for protein kinase enzymes, in *Assay Guid. Man.*, pp. 1–19.

Gong H., Yuan Z., Zhan L. (2016) High-throughput screening against 6.1 million structurally diverse, lead-like compounds to discover novel ROCK inhibitors for cerebral injury recovery. *Mol. Divers.* **20**, 537–549.

Graves B., Thompson T., Xia M., Janson C., Lukacs C., Deo D., Lello P. Di, et al. (2012) Activation of the p53 pathway by small-molecule- induced MDM2 and MDMX dimerization. *Proc. Natl. Acad. Sci. U.S.A.* **109**, 11788–11793.

Gunasekaran K., Tsai C. J., Kumar S., Zanuy D., Nussinov R. (2003) Extended disordered proteins: Targeting function with less scaffold. *Trends Biochem. Sci.* **28**, 81–85.

Hastie C. J., McLauchlan H. J., Cohen P. (2006) Assay of protein kinases using radiolabeled ATP: a protocol. *Nat. Protoc.* **1**, 968–971.

Hidaka H., Hagiwara M., Chijiwa T. (1990) Molecular pharmacology of protein kinases. *Neurochem. Res.* **15**, 431–434.

Honig B., Ray A., Levinthal C. (1976) Conformational flexibility and protein folding: rigid structural fragments connected by flexible joints in subtilisin BPN. *Proc. Natl. Acad. Sci. U. S. A.* **73**, 1974–1978.

Honigberg L. A., Smith A. M., Sirisawad M., Verner E., Loury D., Chang B., Li S., et al. (2010) The Bruton tyrosine kinase inhibitor PCI-32765 blocks B-cell activation and is efficacious in models of autoimmune disease and B-cell malignancy. *Proc. Natl. Acad. Sci.* **107**, 13075–13080.

Huang S., Li Q., Alberts I., Li X. (2016) PRKX, a novel cAMP-dependent protein kinase member, plays an important role in development. *J. Cell. Biochem.* **117**, 566–573.

Huang Xinyi (2003) Fluorescence Polarization Competition Assay: The Range of Resolvable Inhibitor Potency Is Limited by the Affinity of the Fluorescent Ligand. *J. Biomol. Screen.* **8**, 34–38.

Inanami T., Terada T. P., Sasai M. (2014) Folding pathway of a multidomain protein depends on its topology of domain connectivity. *Proc. Natl. Acad. Sci.* **111**, 15969–15974.

Jacobs M., Hayakawa K., Swenson L., Bellon S., Fleming M., Taslimi P., Doran J. (2006) The structure of dimeric ROCK I reveals the mechanism for ligand selectivity. *J. Biol. Chem.* **281**, 260–268.

Jencks W. P. (1981) On the attribution and additivity of binding energies. *Proc. Natl. Acad. Sci. U. S. A.* **78**, 4046–4050.
Jensen O. N. (2004) Modification-specific proteomics: Characterization of post-translational modifications by mass spectrometry. *Curr. Opin. Chem. Biol.* **8**, 33–41.
Khoury G. A., Baliban R. C., Floudas C. A. (2011) Proteome-wide post-translational modification statistics: frequency analysis and curation of the swiss-prot database. *Sci. Rep.* **1**, 90.
Kim M.-S., Pinto S., Getnet D., Nirujogi R., Manda S., Chaerkady R., Madugundu A., et al. (2014) A draft map of the human proteome. *Nature* **509**, 575–581.
Knight J. D. R., Qian B., Baker D., Kothary R. (2007) Conservation, variability and the modeling of active protein kinases. *PLoS One* **2**, e982.
Kraskouskaya D., Duodu E., Arpin C. C., Gunning P. T. (2013) Progress towards the development of SH2 domain inhibitors. *Chem. Soc. Rev.* **42**, 3337.
Kreegipuu A., Blom N., Brunak S., Jarv J. (1998) Statistical analysis of protein kinase specificity determinants. *FEBS Lett.* **430**, 45–50.
Kubelka J., Hofrichter J., Eaton W. A. (2004) The protein folding "speed limit." *Curr. Opin. Struct. Biol.* **14**, 76–88.
Lakowicz J. R. (2006a) Fluorescence Anisotropy, in *Princ. Fluoresc. Spectrosc.*, pp. 353–382. Springer US, Boston, MA.
Lakowicz J. R. (2006b) Energy Transfer, in *Princ. Fluoresc. Spectrosc.*, pp. 443–475. Springer US, Boston, MA.
Lavogina D., Enkvist E., Uri A. (2010a) Bisubstrate inhibitors of protein kinases: from principle to practical applications. *ChemMedChem* **5**, 23–34.
Lavogina D., Lust M., Viil I., König N., Raidaru G., Rogozina J., Enkvist E., Uri A., Bossemeyer D. (2009) Structural analysis of ARC-type inhibitor (ARC-1034) binding to protein kinase A catalytic subunit and rational design of bisubstrate analogue inhibitors of basophilic protein kinases. *J. Med. Chem.* **52**, 308–321.
Lavogina D., Nickl C. K., Enkvist E., Raidaru G., Lust M., Vaasa A., Uri A., Dostmann W. R. (2010b) Adenosine analogue-oligo-arginine conjugates (ARCs) serve as high-affinity inhibitors and fluorescence probes of type I cGMP-dependent protein kinase (PKGIalpha). *Biochim. Biophys. Acta* **1804**, 1857–1868.
Leavitt S., Freire E. (2001) Direct measurement of protein binding energetics by isothermal titration calorimetry. *Curr. Opin. Struct. Biol.* **11**, 560–566.
Lebakken C. S., Riddle S. M., Singh U., Frazee W. J., Eliason H. C., Gao Y., Reichling L. J., Marks B. D., Vogel K. W. (2009) Development and applications of a broad-coverage, TR-FRET-based kinase binding assay platform. *J. Biomol. Screen.* **14**, 924–935.
Leung T., Manser E., Tan L., Lim L. (1995) A novel serine/threonine kinase binding the ras-related RhoA GTPase which translocates the kinase to peripheral membranes. *J. Biol. Chem.* **270**, 29051–29054.
Ligi K., Enkvist E., Uri A. (2016) Deoxygenation increases photoluminescence lifetime of protein-responsive organic probes with triplet-singlet resonant energy transfer. *J. Phys. Chem. B* **120**, 4945–4954.
Lipinski C. A., Lombardo F., Dominy B. W., Feeney P. J. (1997) Experimental and computational approaches to estimate solubility and permeability in drug discovery and development settings. *Adv. Drug Deliv. Rev.* **23**, 3–25.
Lissandron V., Terrin A., Collini M., D'Alfonso L., Chirico G., Pantano S., Zaccolo M. (2005) Improvement of a FRET-based indicator for cAMP by linker design and stabilization of donor-acceptor interaction. *J. Mol. Biol.* **354**, 546–555.

Liu B. A., Engelmann B. W., Jablonowski K., Higginbotham K., Stergachis A. B., Nash P. D. (2012) SRC Homology 2 Domain Binding Sites in Insulin, IGF-1 and FGF receptor mediated signaling networks reveal an extensive potential interactome. *Cell Commun. Signal.* **10**, 27.

Liu B. A., Shah E., Jablonowski K., Stergachis A., Engelmann B., Nash P. D. (2011) The SH2 domain-containing proteins in 21 species establish the provenance and scope of phosphotyrosine signaling in eukaryotes. *Sci. Signal.* **4**, ra83.

Liu Z., Gong Z., Dong X., Tang C. (2016) Transient protein-protein interactions visualized by solution NMR. *Biochim. Biophys. Acta – Proteins Proteomics* **1864**, 115–122.

Loirand G., Touyz R. M. (2015) Rho kinases in health and disease. *Pharmacol Rev* **67**, 1074–1095.

Loog M., Uri A., Raidaru G., Järv J., Ek P. (1999) Adenosine-5'-carboxylic acid peptidyl derivatives as inhibitors of protein kinases. *Bioorg. Med. Chem. Lett.* **9**, 1447–1452.

Lu H., Tonge P. J. (2010) Drug-target residence time: critical information for lead optimization. *Curr. Opin. Chem. Biol.* **14**, 467–474.

Ma H., Horiuchi K. Y., Wang Y., Kucharewicz S. a, Diamond S. L. (2005) Nanoliter homogenous ultra-high throughput screening microarray for lead discoveries and IC50 profiling. *Assay Drug Dev. Technol.* **3**, 177–187.

Macala L. J., Hayslett J. P., Smallwood J. I. (1998) Measurement of cAMP-dependent protein kinase activity using a fluorescent-labeled Kemptide. *Kidney Int.* **54**, 1746–1750.

Mack E. T., Snyder P. W., Perez-Castillejos R., Bilgiçer B., Moustakas D. T., Butte M. J., Whitesides G. M. (2012) Dependence of avidity on linker length for a bivalent ligand-bivalent receptor model system. *J. Am. Chem. Soc.* **134**, 333–345.

Manley P. W., Cowan-Jacob S. W., Buchdunger E., Fabbro D., Fendrich G., Furet P., Meyer T., Zimmermann J. (2002) Imatinib: a selective tyrosine kinase inhibitor. *Eur. J. Cancer* **38**, S19–27.

Manning G. (2002) The Protein Kinase Complement of the Human Genome. *Science (80–.).* **298**, 1912–1934.

Manning G., Whyte D. B., Martinez R., Hunter T., Sudarsanam S. (2002) The protein kinase complement of the human genome. *Science* **298**, 1912–1934.

Markham K., Bai Y., Schmitt-Ulms G. (2007) Co-immunoprecipitations revisited: An update on experimental concepts and their implementation for sensitive interactome investigations of endogenous proteins. *Anal. Bioanal. Chem.* **389**, 461–473.

Meyer-Almes F. J. (2015) Kinetic binding assays for the analysis of protein-ligand interactions. *Drug Discov. Today Technol.* **17**, 1–8.

Mitra R. D., Silva C. M., Youvan D. C. (1996) Fluorescence resonance energy transfer between blue-emitting and red-shifted excitation derivatives of the green fluorescent protein. *Gene* **173**, 13–17.

Miura T., Matsuo A., Muraoka T., Ide M., Morikami K., Kamikawa T., Nishihara M., Kashiwagi H. (2016) Identification of a selective inhibitor of transforming growth factor B-activated kinase 1 by biosensor-based screening of focused libraries. *Bioorganic Med. Chem. Lett.* **27**, 1031–1036.

Morgan-Fisher M., Wewer U. M., Yoneda A. (2013) Regulation of ROCK activity in cancer. *J. Histochem. Cytochem.* **61**, 185–198.

Muñoz V., Eaton W. a (1999) A simple model for calculating the kinetics of protein folding from three-dimensional structures. *Proc. Natl. Acad. Sci. U. S. A.* **96**, 11311–11316.

Nikolovska-Coleska Z., Wang R., Fang X., Pan H., Tomita Y., Li P., Roller P. P., et al. (2004) Development and optimization of a binding assay for the XIAP BIR3 domain using fluorescence polarization. *Anal. Biochem.* **332**, 261–273.

Nim S., Jeon J., Corbi-Verge C., Seo M.-H., Ivarsson Y., Moffat J., Tarasova N., Kim P. M. (2016) Pooled screening for antiproliferative inhibitors of protein-protein interactions. *Nat. Chem. Biol.* **12**, 275–281.

Nishi H., Demir E., Panchenko A. R. (2015) Crosstalk between signaling pathways provided by single and multiple protein phosphorylation sites. *J. Mol. Biol.* **427**, 511–520.

Ofran Y., Rost B. (2003) Analysing six types of protein-protein interfaces. *J. Mol. Biol.* **325**, 377–387.

Olsson T. S. G., Williams M. A., Pitt W. R., Ladbury J. E. (2008) The thermodynamics of protein-ligand interaction and solvation: insights for ligand design. *J. Mol. Biol.* **384**, 1002–1017.

Owicki J. C. (2000) Fluorescence polarization and anisotropy in high throughput screening: Perspectives and primer. *J. Biomol. Screen.* **5**, 297–306.

Paramanathan T., Reeves D., Friedman L. J., Kondev J., Gelles J. (2014) A general mechanism for competitor-induced dissociation of molecular complexes. *Nat. Commun.* **5**, 5207.

Parang K., Till J. H., Ablooglu A. J., Kohanski R. A., Hubbard S. R., Cole P. A. (2001) Mechanism-based design of a protein kinase inhibitor. *Nat. Struct. Biol.* **8**, 37–41.

Pearce L. R., Komander D., Alessi D. R. (2010) The nuts and bolts of AGC protein kinases. *Nat. Rev. Mol. Cell Biol.* **11**, 9–22.

Perozzo R., Folkers G., Scapozza L. (2004) Thermodynamics of protein-ligand interactions: history, presence, and future aspects. *J. Recept. Signal Transduct. Res.* **24**, 1–52.

Petryszak R., Keays M., Tang Y. A., Fonseca N. A., Barrera E., Burdett T., Füllgrabe A., et al. (2016) Expression Atlas update – an integrated database of gene and protein expression in humans, animals and plants. *Nucleic Acids Res.* **44**, D746–D752.

Pflug A., Rogozina J., Lavogina D., Enkvist E., Uri A., Engh R. A., Bossemeyer D. (2010) Diversity of bisubstrate binding modes of adenosine analogue-oligoarginine conjugates in protein kinase a and implications for protein substrate interactions. *J. Mol. Biol.* **403**, 66–77.

Piovesan D., Tabaro F., Micetić I., Necci M., Quaglia F., Oldfield C. J., Aspromonte M. C., et al. (2017) DisProt 7.0: a major update of the database of disordered proteins. *Nucleic Acids Res.* **45**, D219–D227.

Pollard T. D. (2010) A Guide to Simple and Informative Binding Assays. *Mol. Biol. Cell* **21**, 4061–4067.

Rao V. S., Srinivas K., Sujini G. N., Kumar G. N. S. (2014) Protein-Protein Interaction Detection: Methods and Analysis. *Int. J. Proteomics* **2014**, 1–12.

Ren L., Emery D., Kaboord B., Chang E., Qoronfleh M. W. (2003) Improved immunomatrix methods to detect protein:protein interactions. *J. Biochem. Biophys. Methods* **57**, 143–157.

Ricouart A., Gesquiere J. C., Tartar A., Sergheraert C. (1991) Design of potent protein kinase inhibitors using the bisubstrate approach. *J. Med. Chem.* **34**, 73–78.

Rininsland F., Xia W., Wittenburg S., Shi X., Stankewicz C., Achyuthan K., McBranch D., Whitten D. (2004) Metal ion-mediated polymer superquenching for highly sensitive detection of kinase and phosphatase activities. *Proc. Natl. Acad. Sci. U. S. A.* **101**, 15295–15300.

Rolland T., Tasan M., Charloteaux B., Pevzner S. J., Zhong Q., Sahni N., Yi S., et al. (2014) A proteome-scale map of the human interactome network. *Cell* **159**, 1212–1226.

Roth G. J., Majerus P. W. (1975) The mechanism of the effect of aspirin on human platelets. I. Acetylation of a particulate fraction protein. *J. Clin. Invest.* **56**, 624–632.

Santos R., Ursu O., Gaulton A., Bento A. P., Donadi R. S., Bologa C. G., Karlsson A., et al. (2016) A comprehensive map of molecular drug targets. *Nat. Rev. Drug Discov.* **16**, 19–34.

Sarbassov D. D. (2005) Phosphorylation and Regulation of Akt/PKB by the Rictor-mTOR Complex. *Science (80–.).* **307**, 1098–1101.

Scheibner K. A., Zhang Z., Cole P. A. (2003) Merging fluorescence resonance energy transfer and expressed protein ligation to analyze protein-protein interactions. *Anal. Biochem.* **317**, 226–232.

Schenk P. W., Snaar-Jagalska B. E. (1999) Signal perception and transduction: The role of protein kinases. *Biochim. Biophys. Acta – Mol. Cell Res.* **1449**, 1–24.

Schofield A. V., Gamell C., Suryadinata R., Sarcevic B., Bernard O. (2013) Tubulin polymerization promoting protein 1 (Tppp1) Phosphorylation by Rho-associated coiled-coil kinase (Rock) and cyclin-dependent kinase 1 (Cdk1) inhibits microtubule dynamics to increase cell proliferation. *J. Biol. Chem.* **288**, 7907–7917.

Shaw M., Cohen P., Alessi D. R. (1997) Further evidence that the inhibition of glycogen synthase kinase-3β by IGF-1 is mediated by PDK1/PKB-induced phosphorylation of Ser-9 and not by dephosphorylation of Tyr-216. *FEBS Lett.* **416**, 307–311.

Spencer D. M., Wandless T. J., Schreiber S. L., Crabtree G. R. (1993) Controlling signal transduction with synthetic ligands. *Science* **262**, 1019–1024.

Sprinzak E., Sattath S., Margalit H. (2003) How reliable are experimental protein-protein interaction data? *J. Mol. Biol.* **327**, 919–923.

Stenroos K., Hurskainen P., Eriksson S., Hemmilä I., Blomberg K., Lindqvist C. (1998) Homogeneous time-resolved IL-2–IL-2Rα assay using fluroescence resonance energy transfer. *Cytokine* **10**, 495–499.

Stull J. T., Kamm K. E., Vandenboom R. (2011) Myosin light chain kinase and the role of myosin light chain phosphorylation in skeletal muscle. *Arch. Biochem. Biophys.* **510**, 120–128.

Sugase K., Dyson H. J., Wright P. E. (2007) Mechanism of coupled folding and binding of an intrinsically disordered protein. *Nature* **447**, 1021–1025.

Zaccolo M., Giorgi F. De, Cho C. Y., Feng L., Knapp T., Negulescu P. A., Taylor S. S., Tsien R. Y., Pozzan T. (2000) A genetically encoded, fluorescent indicator for cyclic AMP in living cells. *Nat. Cell Biol.* **2**, 25–29.

Zhang H., Tang X., Munske G. R., Tolic N., Anderson G. A., Bruce J. E. (2009) Identification of Protein-Protein Interactions and Topologies in Living Cells with Chemical Cross-linking and Mass Spectrometry. *Mol. Cell. Proteomics* **8**, 409–420.

Zhang H., Wu Q., Berezin M. Y. (2015) Fluorescence anisotropy (polarization): from drug screening to precision medicine. *Expert Opin. Drug Discov.* **10**, 1145–1161.

Zhang L., Duan C. J., Binkley C., Li G., Uhler M. D., Logsdon C. D., Simeone D. M. (2004) A transforming growth factor beta-induced Smad3/Smad4 complex directly activates protein kinase A. *Mol. Cell. Biol.* **24**, 2169–2180.

Zhong H., SuYang H., Erdjument-Bromage H., Tempst P., Ghosh S. (1997) The transcriptional activity of NF-kB is regulated by the IkB- associated PKAc subunit through a cyclic AMP-independent mechanism. *Cell* **89**, 413–424.

Zhou L., Fang C., Wei P., Liu S., Liu Y., Lai L. (2008) Chemically induced dimerization of human nonpancreatic secretory phospholipase A2 by bis-indole derivatives. *J. Med. Chem.* **51**, 3360–3366.

Taylor S. S., Yang J., Wu J., Haste N. M., Radzio-Andzelm E., Anand G. (2004) PKA: A portrait of protein kinase dynamics. *Biochim. Biophys. Acta – Proteins Proteomics* **1697**, 259–269.

Terrin A., Monterisi S., Stangherlin A., Zoccarato A., Koschinski A., Surdo N. C., Mongillo M., et al. (2012) PKA and PDE4D3 anchoring to AKAP9 provides distinct regulation of cAMP signals at the centrosome. *J. Cell Biol.* **198**, 607–621.

Theillet F.-X., Binolfi A., Frembgen-Kesner T., Hingorani K., Sarkar M., Kyne C., Li C., et al. (2014) Physicochemical properties of cells and their effects on intrinsically disordered proteins (IDPs). *Chem. Rev.* **114**, 6661–6714.

Thiel P., Kaiser M., Ottmann C. (2012) Small-molecule stabilization of protein-protein interactions: An underestimated concept in drug discovery? *Angew. Chemie – Int. Ed.* **51**, 2012–2018.

Tillo S. E., Xiong W. H., Takahashi M., Miao S., Andrade A. L., Fortin D. A., Yang G., et al. (2017) Liberated PKA catalytic subunits associate with the membrane via myristoylation to preferentially phosphorylate membrane substrates. *Cell Rep.* **19**, 617–629.

Tummino P. J., Copeland R. A. (2008) Residence time of receptor-ligand complexes and its effect on biological function. *Biochemistry* **47**, 5481–5492.

Turnham R. E., Scott J. D. (2017) Protein kinase A catalytic subunit isoform PRKACA; history, function and physiology. **577**, 101–108.

Tönges L., Frank T., Tatenhorst L., Saal K. A., Koch J. C., Szego E. M., Bahr M., Weishaupt J. H., Lingor P. (2012) Inhibition of rho kinase enhances survival of dopaminergic neurons and attenuates axonal loss in a mouse model of Parkinson's disease. *Brain* **135**, 3355–3370.

Újvári A., Aron R., Eisenhaure T., Cheng E., Parag H. A., Smicun Y., Halaban R., Hebert D. N. (2001) Translation rate of human tyrosinase determines its N-linked glycosylation level. *J. Biol. Chem.* **276**, 5924–5931.

Uri A., Raidaru G., Subbi J., Padari K., Pooga M. (2002) Identification of the ability of highly charged nanomolar inhibitors of protein kinases to cross plasma membranes and carry a protein into cells. *Bioorg. Med. Chem. Lett.* **12**, 2117–2120.

Vaasa A., Viil I., Enkvist E., Viht K., Raidaru G., Lavogina D., Uri A. (2009) High-affinity bisubstrate probe for fluorescence anisotropy binding/displacement assays with protein kinases PKA and ROCK. *Anal. Biochem.* **385**, 85–93.

Wako H., Saito N. (1978) Statistical Mechanical Theory of the Protein Conformation. II. Folding Pathway for Protein. *J. Phys. Soc. Japan* **44**, 1939–1945.

Vauquelin G., Liefde I. Van (2012) Radioligand dissociation measurements: potential interference of rebinding and allosteric mechanisms and physiological relevance of the biological model systems. *Expert Opin. Drug Discov.* **7**, 583–595.

Wells J. A., McClendon C. L. (2007) Reaching for high-hanging fruit in drug discovery at protein-protein interfaces. *Nature* **450**, 1001–1009.

Viht K., Schweinsberg S., Lust M., Vaasa A., Raidaru G., Lavogina D., Uri A., Herberg F. W. (2007) Surface-plasmon-resonance-based biosensor with immobilized bisubstrate analog inhibitor for the determination of affinities of ATP- and protein-competitive ligands of cAMP-dependent protein kinase. *Anal. Biochem.* **362**, 268–277.

Viht K., Vaasa A., Raidaru G., Enkvist E., Uri A. (2005) Fluorometric TLC assay for evaluation of protein kinase inhibitors. *Anal. Biochem.* **340**, 165–170.
Wiseman T., Williston S., Brandts J. F., Lin L.-N. (1989) Rapid measurement of binding constants and heats of binding using a new titration calorimeter. *Anal. Biochem.* **179**, 131–137.
Witt J. J., Roskoski R. (1975) Rapid protein kinase assay using phosphocellulose-paper absorption. *Anal. Biochem.* **66**, 253–258.
Wittig I., Schägger H. (2009) Native electrophoretic techniques to identify protein-protein interactions. *Proteomics* **9**, 5214–5223.
Vlastaridis P., Kyriakidou P., Chaliotis A., Peer Y. Van de, Oliver S. G., Amoutzias G. D. (2017) Estimating the total number of phosphoproteins and phosphorylation sites in eukaryotic proteomes. *Gigascience* **6**, 1–11.
Wu P., Nielsen T. E., Clausen M. H. (2016) Small-molecule kinase inhibitors: An analysis of FDA-approved drugs. *Drug Discov. Today* **21**, 5–10.
Yan C., Wu F., Jernigan R. L., Dobbs D. (2008) NIH Public Access. *October* **27**, 59–70.
Yang G., Zhou Y., Liu X., Xu L., Cao Y., Manning R. J., Patterson C. J., et al. (2013) A mutation in MYD88 (L265P) supports the survival of lymphoplasmacytic cells by activation of Bruton tyrosine kinase in Waldenström macroglobulinemia. *Blood* **122**, 1222–1232.
Yang J., Cron P., Good V. M., Thompson V., Hemmings B. A., Barford D. (2002) Crystal structure of an activated Akt/Protein Kinase B ternary complex with GSK3-peptide and AMP-PNP. *Nat. Struct. Biol.* **9**, 940–944.
Yoeli-Lerner M., Toker A., Israel B. (2006) Akt/PKB signaling in cancer: A function in cell motility and invasion. *Cell Cycle* **6036**, 603–605.

ACKNOWLEDGEMENTS

First, I would like to thank the nature itself for being a complicated system. It seems that there will be no end in resolving some of the most intriguing tasks, and even simpler endeavors can be left without an answer. It is fascinating, really, and relatively frustrating simultaneously.

I express sincere gratitude to my supervisor Asko. He has been a splendid example of the researcher with concrete scope, knowing to focus on what is important. I have enjoyed the discussions we have had, both on professional and casual topics. The amount of patience Asko has shown during the tough times is admirable and I wish that there will be easier times ahead.

One could not wish for better labmates. The unbelievably high knowledge- and logic-driven guidance from Erki, innovative yet simple ideas from Kaido, vast experience-based tips from Darja, and of course, immeasurable help from Angela and Marje made the 8 years in laboratory worth remembering. I enjoyed the company of Marie, Jürgen, and Kadri, who had to put up with me for years. It was a pleasure to work with my students Hegne, Anna, and Sylvestre.

Of special note, we grew very close with Hedi. She is a person one should really make friends with. Hedi is the most sincere, helpful, and rational individual at the same time, and I should really take note of her organizational abilities.

To mention the bioorganic chemistry chair, my thanks go to Ago, Sergei, Olga, Anni, Kerli, Taavi, and Reet, because we spent some good times together and supported each other wherever possible. I would also like to thank professor Richard Alan Engh, who has always been very relaxed and gave me the opportunity to broaden my views about crystallography in Tromsø. Bjarte and Kazi helped me a lot to settle in the soft weather of Norway and thank you for that. Though we have never met in person, the conversations with Alexander have been most fruitful, his recommendations are a part of this thesis and I am grateful for his observations.

I would like to thank my friends, especially Akis, Mari-Liis, and Jaanika, and family. Despite we do not see much, I am thinking of you at times.

Last but not least, there is no greater pleasure to mention Ene-Ly here. The way our paths crossed again is written but hidden somewhere in the laws of physics and chemistry.

PUBLICATIONS

CURRICULUM VITAE

Name: Taavi Ivan
Date of Birth: August 7, 1989
Citizenship: Estonian
Address: University of Tartu, Institute of Chemistry, Ravila 14a, 50411, Tartu, Estonia
e-mail: taavi.ivan@ut.ee

Education

2013 – … University of Tartu, PhD student in chemistry
2011 – 2013 University of Tartu, MSc in chemistry
2008 – 2011 University of Tartu, BSc in chemistry

Professional self-improvement

2012 Protein production, purification, co-crystallization of ARC-type inhibitors with PKAc, and thermodynamic characterization of ARC-type inhibitors in complex with protein kinases; University of Tromsø, Norway

Scientific publications

E. Enkvist, A. Vaasa, M. Kasari, M. Kriisa, **T. Ivan**, K. Ligi, G. Raidaru, A. Uri, Protein-induced long lifetime luminescence of nonmetal probes, ACS Chem. Biol. 6 (2011) 1052–1062.

T. Ivan, E. Enkvist, B. Viira, G.B. Manoharan, G. Raidaru, A. Pflug, K.A. Alam, M. Zaccolo, R.A. Engh, A. Uri, Bifunctional ligands for inhibition of tight-binding protein-protein interactions, Bioconjug. Chem. 27 (2016) 1900–1910.

H. Sinijarv, S. Wu, **T. Ivan**, T. Laasfeld, K. Viht, A. Uri, Binding assay for characterization of protein kinase inhibitors possessing sub-picomolar to sub-millimolar affinity, Anal. Biochem. 531 (2017) 67–77.

T. Ivan, E. Enkvist, H. Sinijarv, A. Uri, Competitive ligands facilitate dissociation of the complex of bifunctional inhibitor and protein kinase, Biophys. Chem. 228 (2017) 17–24.

ELULOOKIRJELDUS

Nimi: Taavi Ivan
Sünniaeg: August 7, 1989
Kodakondsus: Eesti
Aadress: Tartu Ülikool, keemia instituut, Ravila 14a, 50411, Tartu, Eesti
E-mail: taavi.ivan@ut.ee

Hariduskäik

2013 – … Tartu Ülikool, doktoriõpe keemias
2011 – 2013 Tartu Ülikool, MSc keemias
2008 – 2011 Tartu Ülikool, BSc keemias

Erialane enesetäiendus

2012 Valkude tootmine, puhastamine, kooskristallimine ARC-põhiste inhibiitoritega ja ARC:proteiinkinaas komplekside termodünaamiliste parameetrite mõõtmine; Tromsø Ülikool, Norra

Teaduspublikatsioonid

E. Enkvist, A. Vaasa, M. Kasari, M. Kriisa, **T. Ivan**, K. Ligi, G. Raidaru, A. Uri, Protein-induced long lifetime luminescence of nonmetal probes., ACS Chem. Biol. 6 (2011) 1052–1062.

T. Ivan, E. Enkvist, B. Viira, G.B. Manoharan, G. Raidaru, A. Pflug, K.A. Alam, M. Zaccolo, R.A. Engh, A. Uri, Bifunctional ligands for inhibition of tight-binding protein-protein interactions, Bioconjug. Chem. 27 (2016) 1900–1910.

H. Sinijarv, S. Wu, **T. Ivan**, K. Viht, A. Uri, Binding assay for characterization of protein kinase inhibitors possessing sub-picomolar to sub-millimolar affinity, Anal. Biochem. (2017).

T. Ivan, E. Enkvist, H. Sinijarv, A. Uri, Competitive ligands facilitate dissociation of the complex of bifunctional inhibitor and protein kinase, Biophys. Chem. 228 (2017) 17–24.

DISSERTATIONES CHIMICAE UNIVERSITATIS TARTUENSIS

1. **Toomas Tamm.** Quantum-chemical simulation of solvent effects. Tartu, 1993, 110 p.
2. **Peeter Burk.** Theoretical study of gas-phase acid-base equilibria. Tartu, 1994, 96 p.
3. **Victor Lobanov.** Quantitative structure-property relationships in large descriptor spaces. Tartu, 1995, 135 p.
4. **Vahur Mäemets.** The ^{17}O and ^{1}H nuclear magnetic resonance study of H_2O in individual solvents and its charged clusters in aqueous solutions of electrolytes. Tartu, 1997, 140 p.
5. **Andrus Metsala.** Microcanonical rate constant in nonequilibrium distribution of vibrational energy and in restricted intramolecular vibrational energy redistribution on the basis of slater's theory of unimolecular reactions. Tartu, 1997, 150 p.
6. **Uko Maran.** Quantum-mechanical study of potential energy surfaces in different environments. Tartu, 1997, 137 p.
7. **Alar Jänes.** Adsorption of organic compounds on antimony, bismuth and cadmium electrodes. Tartu, 1998, 219 p.
8. **Kaido Tammeveski.** Oxygen electroreduction on thin platinum films and the electrochemical detection of superoxide anion. Tartu, 1998, 139 p.
9. **Ivo Leito.** Studies of Brønsted acid-base equilibria in water and non-aqueous media. Tartu, 1998, 101 p.
10. **Jaan Leis.** Conformational dynamics and equilibria in amides. Tartu, 1998, 131 p.
11. **Toonika Rinken.** The modelling of amperometric biosensors based on oxidoreductases. Tartu, 2000, 108 p.
12. **Dmitri Panov.** Partially solvated Grignard reagents. Tartu, 2000, 64 p.
13. **Kaja Orupõld.** Treatment and analysis of phenolic wastewater with microorganisms. Tartu, 2000, 123 p.
14. **Jüri Ivask.** Ion Chromatographic determination of major anions and cations in polar ice core. Tartu, 2000, 85 p.
15. **Lauri Vares.** Stereoselective Synthesis of Tetrahydrofuran and Tetrahydropyran Derivatives by Use of Asymmetric Horner-Wadsworth-Emmons and Ring Closure Reactions. Tartu, 2000, 184 p.
16. **Martin Lepiku.** Kinetic aspects of dopamine D_2 receptor interactions with specific ligands. Tartu, 2000, 81 p.
17. **Katrin Sak.** Some aspects of ligand specificity of P2Y receptors. Tartu, 2000, 106 p.
18. **Vello Pällin.** The role of solvation in the formation of iotsitch complexes. Tartu, 2001, 95 p.
19. **Katrin Kollist.** Interactions between polycyclic aromatic compounds and humic substances. Tartu, 2001, 93 p.

20. **Ivar Koppel.** Quantum chemical study of acidity of strong and superstrong Brønsted acids. Tartu, 2001, 104 p.
21. **Viljar Pihl.** The study of the substituent and solvent effects on the acidity of OH and CH acids. Tartu, 2001, 132 p.
22. **Natalia Palm.** Specification of the minimum, sufficient and significant set of descriptors for general description of solvent effects. Tartu, 2001, 134 p.
23. **Sulev Sild.** QSPR/QSAR approaches for complex molecular systems. Tartu, 2001, 134 p.
24. **Ruslan Petrukhin.** Industrial applications of the quantitative structure-property relationships. Tartu, 2001, 162 p.
25. **Boris V. Rogovoy.** Synthesis of (benzotriazolyl)carboximidamides and their application in relations with *N*- and *S*-nucleophyles. Tartu, 2002, 84 p.
26. **Koit Herodes.** Solvent effects on UV-vis absorption spectra of some solvatochromic substances in binary solvent mixtures: the preferential solvation model. Tartu, 2002, 102 p.
27. **Anti Perkson.** Synthesis and characterisation of nanostructured carbon. Tartu, 2002, 152 p.
28. **Ivari Kaljurand.** Self-consistent acidity scales of neutral and cationic Brønsted acids in acetonitrile and tetrahydrofuran. Tartu, 2003, 108 p.
29. **Karmen Lust.** Adsorption of anions on bismuth single crystal electrodes. Tartu, 2003, 128 p.
30. **Mare Piirsalu.** Substituent, temperature and solvent effects on the alkaline hydrolysis of substituted phenyl and alkyl esters of benzoic acid. Tartu, 2003, 156 p.
31. **Meeri Sassian.** Reactions of partially solvated Grignard reagents. Tartu, 2003, 78 p.
32. **Tarmo Tamm.** Quantum chemical modelling of polypyrrole. Tartu, 2003. 100 p.
33. **Erik Teinemaa.** The environmental fate of the particulate matter and organic pollutants from an oil shale power plant. Tartu, 2003. 102 p.
34. **Jaana Tammiku-Taul.** Quantum chemical study of the properties of Grignard reagents. Tartu, 2003. 120 p.
35. **Andre Lomaka.** Biomedical applications of predictive computational chemistry. Tartu, 2003. 132 p.
36. **Kostyantyn Kirichenko.** Benzotriazole – Mediated Carbon–Carbon Bond Formation. Tartu, 2003. 132 p.
37. **Gunnar Nurk.** Adsorption kinetics of some organic compounds on bismuth single crystal electrodes. Tartu, 2003, 170 p.
38. **Mati Arulepp.** Electrochemical characteristics of porous carbon materials and electrical double layer capacitors. Tartu, 2003, 196 p.
39. **Dan Cornel Fara.** QSPR modeling of complexation and distribution of organic compounds. Tartu, 2004, 126 p.
40. **Riina Mahlapuu.** Signalling of galanin and amyloid precursor protein through adenylate cyclase. Tartu, 2004, 124 p.

41. **Mihkel Kerikmäe.** Some luminescent materials for dosimetric applications and physical research. Tartu, 2004, 143 p.
42. **Jaanus Kruusma.** Determination of some important trace metal ions in human blood. Tartu, 2004, 115 p.
43. **Urmas Johanson.** Investigations of the electrochemical properties of polypyrrole modified electrodes. Tartu, 2004, 91 p.
44. **Kaido Sillar.** Computational study of the acid sites in zeolite ZSM-5. Tartu, 2004, 80 p.
45. **Aldo Oras.** Kinetic aspects of dATPαS interaction with $P2Y_1$ receptor. Tartu, 2004, 75 p.
46. **Erik Mölder.** Measurement of the oxygen mass transfer through the air-water interface. Tartu, 2005, 73 p.
47. **Thomas Thomberg.** The kinetics of electroreduction of peroxodisulfate anion on cadmium (0001) single crystal electrode. Tartu, 2005, 95 p.
48. **Olavi Loog.** Aspects of condensations of carbonyl compounds and their imine analogues. Tartu, 2005, 83 p.
49. **Siim Salmar.** Effect of ultrasound on ester hydrolysis in aqueous ethanol. Tartu, 2006, 73 p.
50. **Ain Uustare.** Modulation of signal transduction of heptahelical receptors by other receptors and G proteins. Tartu, 2006, 121 p.
51. **Sergei Yurchenko.** Determination of some carcinogenic contaminants in food. Tartu, 2006, 143 p.
52. **Kaido Tämm.** QSPR modeling of some properties of organic compounds. Tartu, 2006, 67 p.
53. **Olga Tšubrik.** New methods in the synthesis of multisubstituted hydrazines. Tartu. 2006, 183 p.
54. **Lilli Sooväli.** Spectrophotometric measurements and their uncertainty in chemical analysis and dissociation constant measurements. Tartu, 2006, 125 p.
55. **Eve Koort.** Uncertainty estimation of potentiometrically measured ph and pK_a values. Tartu, 2006, 139 p.
56. **Sergei Kopanchuk.** Regulation of ligand binding to melanocortin receptor subtypes. Tartu, 2006, 119 p.
57. **Silvar Kallip.** Surface structure of some bismuth and antimony single crystal electrodes. Tartu, 2006, 107 p.
58. **Kristjan Saal.** Surface silanization and its application in biomolecule coupling. Tartu, 2006, 77 p.
59. **Tanel Tätte.** High viscosity $Sn(OBu)_4$ oligomeric concentrates and their applications in technology. Tartu, 2006, 91 p.
60. **Dimitar Atanasov Dobchev**. Robust QSAR methods for the prediction of properties from molecular structure. Tartu, 2006, 118 p.
61. **Hannes Hagu**. Impact of ultrasound on hydrophobic interactions in solutions. Tartu, 2007, 81 p.

62. **Rutha Jäger.** Electroreduction of peroxodisulfate anion on bismuth electrodes. Tartu, 2007, 142 p.
63. **Kaido Viht.** Immobilizable bisubstrate-analogue inhibitors of basophilic protein kinases: development and application in biosensors. Tartu, 2007, 88 p.
64. **Eva-Ingrid Rõõm.** Acid-base equilibria in nonpolar media. Tartu, 2007, 156 p.
65. **Sven Tamp.** DFT study of the cesium cation containing complexes relevant to the cesium cation binding by the humic acids. Tartu, 2007, 102 p.
66. **Jaak Nerut.** Electroreduction of hexacyanoferrate(III) anion on Cadmium (0001) single crystal electrode. Tartu, 2007, 180 p.
67. **Lauri Jalukse.** Measurement uncertainty estimation in amperometric dissolved oxygen concentration measurement. Tartu, 2007, 112 p.
68. **Aime Lust.** Charge state of dopants and ordered clusters formation in CaF_2:Mn and CaF_2:Eu luminophors. Tartu, 2007, 100 p.
69. **Iiris Kahn**. Quantitative Structure-Activity Relationships of environmentally relevant properties. Tartu, 2007, 98 p.
70. **Mari Reinik.** Nitrates, nitrites, N-nitrosamines and polycyclic aromatic hydrocarbons in food: analytical methods, occurrence and dietary intake. Tartu, 2007, 172 p.
71. **Heili Kasuk.** Thermodynamic parameters and adsorption kinetics of organic compounds forming the compact adsorption layer at Bi single crystal electrodes. Tartu, 2007, 212 p.
72. **Erki Enkvist.** Synthesis of adenosine-peptide conjugates for biological applications. Tartu, 2007, 114 p.
73. **Svetoslav Hristov Slavov**. Biomedical applications of the QSAR approach. Tartu, 2007, 146 p.
74. **Eneli Härk.** Electroreduction of complex cations on electrochemically polished Bi(*hkl*) single crystal electrodes. Tartu, 2008, 158 p.
75. **Priit Möller.** Electrochemical characteristics of some cathodes for medium temperature solid oxide fuel cells, synthesized by solid state reaction technique. Tartu, 2008, 90 p.
76. **Signe Viggor.** Impact of biochemical parameters of genetically different pseudomonads at the degradation of phenolic compounds. Tartu, 2008, 122 p.
77. **Ave Sarapuu.** Electrochemical reduction of oxygen on quinone-modified carbon electrodes and on thin films of platinum and gold. Tartu, 2008, 134 p.
78. **Agnes Kütt.** Studies of acid-base equilibria in non-aqueous media. Tartu, 2008, 198 p.
79. **Rouvim Kadis.** Evaluation of measurement uncertainty in analytical chemistry: related concepts and some points of misinterpretation. Tartu, 2008, 118 p.
80. **Valter Reedo.** Elaboration of IVB group metal oxide structures and their possible applications. Tartu, 2008, 98 p.

81. **Aleksei Kuznetsov.** Allosteric effects in reactions catalyzed by the cAMP-dependent protein kinase catalytic subunit. Tartu, 2009, 133 p.
82. **Aleksei Bredihhin.** Use of mono- and polyanions in the synthesis of multisubstituted hydrazine derivatives. Tartu, 2009, 105 p.
83. **Anu Ploom.** Quantitative structure-reactivity analysis in organosilicon chemistry. Tartu, 2009, 99 p.
84. **Argo Vonk.** Determination of adenosine A_{2A}- and dopamine D_1 receptor-specific modulation of adenylate cyclase activity in rat striatum. Tartu, 2009, 129 p.
85. **Indrek Kivi.** Synthesis and electrochemical characterization of porous cathode materials for intermediate temperature solid oxide fuel cells. Tartu, 2009, 177 p.
86. **Jaanus Eskusson.** Synthesis and characterisation of diamond-like carbon thin films prepared by pulsed laser deposition method. Tartu, 2009, 117 p.
87. **Marko Lätt.** Carbide derived microporous carbon and electrical double layer capacitors. Tartu, 2009, 107 p.
88. **Vladimir Stepanov.** Slow conformational changes in dopamine transporter interaction with its ligands. Tartu, 2009, 103 p.
89. **Aleksander Trummal.** Computational Study of Structural and Solvent Effects on Acidities of Some Brønsted Acids. Tartu, 2009, 103 p.
90. **Eerold Vellemäe.** Applications of mischmetal in organic synthesis. Tartu, 2009, 93 p.
91. **Sven Parkel.** Ligand binding to 5-HT_{1A} receptors and its regulation by Mg^{2+} and Mn^{2+}. Tartu, 2010, 99 p.
92. **Signe Vahur.** Expanding the possibilities of ATR-FT-IR spectroscopy in determination of inorganic pigments. Tartu, 2010, 184 p.
93. **Tavo Romann**. Preparation and surface modification of bismuth thin film, porous, and microelectrodes. Tartu, 2010, 155 p.
94. **Nadežda Aleksejeva.** Electrocatalytic reduction of oxygen on carbon nanotube-based nanocomposite materials. Tartu, 2010, 147 p.
95. **Marko Kullapere.** Electrochemical properties of glassy carbon, nickel and gold electrodes modified with aryl groups. Tartu, 2010, 233 p.
96. **Liis Siinor.** Adsorption kinetics of ions at Bi single crystal planes from aqueous electrolyte solutions and room-temperature ionic liquids. Tartu, 2010, 101 p.
97. **Angela Vaasa.** Development of fluorescence-based kinetic and binding assays for characterization of protein kinases and their inhibitors. Tartu 2010, 101 p.
98. **Indrek Tulp.** Multivariate analysis of chemical and biological properties. Tartu 2010, 105 p.
99. **Aare Selberg.** Evaluation of environmental quality in Northern Estonia by the analysis of leachate. Tartu 2010, 117 p.
100. **Darja Lavõgina.** Development of protein kinase inhibitors based on adenosine analogue-oligoarginine conjugates. Tartu 2010, 248 p.

101. **Laura Herm.** Biochemistry of dopamine D_2 receptors and its association with motivated behaviour. Tartu 2010, 156 p.
102. **Terje Raudsepp.** Influence of dopant anions on the electrochemical properties of polypyrrole films. Tartu 2010, 112 p.
103. **Margus Marandi.** Electroformation of Polypyrrole Films: *In-situ* AFM and STM Study. Tartu 2011, 116 p.
104. **Kairi Kivirand.** Diamine oxidase-based biosensors: construction and working principles. Tartu, 2011, 140 p.
105. **Anneli Kruve.** Matrix effects in liquid-chromatography electrospray mass-spectrometry. Tartu, 2011, 156 p.
106. **Gary Urb.** Assessment of environmental impact of oil shale fly ash from PF and CFB combustion. Tartu, 2011, 108 p.
107. **Nikita Oskolkov.** A novel strategy for peptide-mediated cellular delivery and induction of endosomal escape. Tartu, 2011, 106 p.
108. **Dana Martin.** The QSPR/QSAR approach for the prediction of properties of fullerene derivatives. Tartu, 2011, 98 p.
109. **Säde Viirlaid.** Novel glutathione analogues and their antioxidant activity. Tartu, 2011, 106 p.
110. **Ülis Sõukand.** Simultaneous adsorption of Cd^{2+}, Ni^{2+}, and Pb^{2+} on peat. Tartu, 2011, 124 p.
111. **Lauri Lipping.** The acidity of strong and superstrong Brønsted acids, an outreach for the "limits of growth": a quantum chemical study. Tartu, 2011, 124 p.
112. **Heisi Kurig.** Electrical double-layer capacitors based on ionic liquids as electrolytes. Tartu, 2011, 146 p.
113. **Marje Kasari.** Bisubstrate luminescent probes, optical sensors and affinity adsorbents for measurement of active protein kinases in biological samples. Tartu, 2012, 126 p.
114. **Kalev Takkis.** Virtual screening of chemical databases for bioactive molecules. Tartu, 2012, 122 p.
115. **Ksenija Kisseljova**. Synthesis of aza-β^3-amino acid containing peptides and kinetic study of their phosphorylation by protein kinase A. Tartu, 2012, 104 p.
116. **Riin Rebane.** Advanced method development strategy for derivatization LC/ESI/MS. Tartu, 2012, 184 p.
117. **Vladislav Ivaništšev.** Double layer structure and adsorption kinetics of ions at metal electrodes in room temperature ionic liquids. Tartu, 2012, 128 p.
118. **Irja Helm.** High accuracy gravimetric Winkler method for determination of dissolved oxygen. Tartu, 2012, 139 p.
119. **Karin Kipper.** Fluoroalcohols as Components of LC-ESI-MS Eluents: Usage and Applications. Tartu, 2012, 164 p.
120. **Arno Ratas.** Energy storage and transfer in dosimetric luminescent materials. Tartu, 2012, 163 p.

121. **Reet Reinart-Okugbeni**. Assay systems for characterisation of subtype-selective binding and functional activity of ligands on dopamine receptors. Tartu, 2012, 159 p.
122. **Lauri Sikk.** Computational study of the Sonogashira cross-coupling reaction. Tartu, 2012, 81 p.
123. **Karita Raudkivi.** Neurochemical studies on inter-individual differences in affect-related behaviour of the laboratory rat. Tartu, 2012, 161 p.
124. **Indrek Saar.** Design of GalR2 subtype specific ligands: their role in depression-like behavior and feeding regulation. Tartu, 2013, 126 p.
125. **Ann Laheäär.** Electrochemical characterization of alkali metal salt based non-aqueous electrolytes for supercapacitors. Tartu, 2013, 127 p.
126. **Kerli Tõnurist.** Influence of electrospun separator materials properties on electrochemical performance of electrical double-layer capacitors. Tartu, 2013, 147 p.
127. **Kaija Põhako-Esko.** Novel organic and inorganic ionogels: preparation and characterization. Tartu, 2013, 124 p.
128. **Ivar Kruusenberg.** Electroreduction of oxygen on carbon nanomaterial-based catalysts. Tartu, 2013, 191 p.
129. **Sander Piiskop.** Kinetic effects of ultrasound in aqueous acetonitrile solutions. Tartu, 2013, 95 p.
130. **Ilona Faustova**. Regulatory role of L-type pyruvate kinase N-terminal domain. Tartu, 2013, 109 p.
131. **Kadi Tamm.** Synthesis and characterization of the micro-mesoporous anode materials and testing of the medium temperature solid oxide fuel cell single cells. Tartu, 2013, 138 p.
132. **Iva Bozhidarova Stoyanova-Slavova.** Validation of QSAR/QSPR for regulatory purposes. Tartu, 2013, 109 p.
133. **Vitali Grozovski**. Adsorption of organic molecules at single crystal electrodes studied by *in situ* STM method. Tartu, 2014, 146 p.
134. **Santa Veikšina**. Development of assay systems for characterisation of ligand binding properties to melanocortin 4 receptors. Tartu, 2014, 151 p.
135. **Jüri Liiv.** PVDF (polyvinylidene difluoride) as material for active element of twisting-ball displays. Tartu, 2014, 111 p.
136. **Kersti Vaarmets.** Electrochemical and physical characterization of pristine and activated molybdenum carbide-derived carbon electrodes for the oxygen electroreduction reaction. Tartu, 2014, 131 p.
137. **Lauri Tõntson**. Regulation of G-protein subtypes by receptors, guanine nucleotides and Mn^{2+}. Tartu, 2014, 105 p.
138. **Aiko Adamson.** Properties of amine-boranes and phosphorus analogues in the gas phase. Tartu, 2014, 78 p.
139. **Elo Kibena**. Electrochemical grafting of glassy carbon, gold, highly oriented pyrolytic graphite and chemical vapour deposition-grown graphene electrodes by diazonium reduction method. Tartu, 2014, 184 p.

140. **Teemu Näykki.** Novel Tools for Water Quality Monitoring – From Field to Laboratory. Tartu, 2014, 202 p.
141. **Karl Kaupmees.** Acidity and basicity in non-aqueous media: importance of solvent properties and purity. Tartu, 2014, 128 p.
142. **Oleg Lebedev**. Hydrazine polyanions: different strategies in the synthesis of heterocycles. Tartu, 2015, 118 p.
143. **Geven Piir.** Environmental risk assessment of chemicals using QSAR methods. Tartu, 2015, 123 p.
144. **Olga Mazina.** Development and application of the biosensor assay for measurements of cyclic adenosine monophosphate in studies of G protein-coupled receptor signalinga. Tartu, 2015, 116 p.
145. **Sandip Ashokrao Kadam.** Anion receptors: synthesis and accurate binding measurements. Tartu, 2015, 116 p.
146. **Indrek Tallo.** Synthesis and characterization of new micro-mesoporous carbide derived carbon materials for high energy and power density electrical double layer capacitors. Tartu, 2015, 148 p.
147. **Heiki Erikson.** Electrochemical reduction of oxygen on nanostructured palladium and gold catalysts. Tartu, 2015, 204 p.
148. **Erik Anderson.** *In situ* Scanning Tunnelling Microscopy studies of the interfacial structure between Bi(111) electrode and a room temperature ionic liquid. Tartu, 2015, 118 p.
149. **Girinath G. Pillai.** Computational Modelling of Diverse Chemical, Bio-chemical and Biomedical Properties. Tartu, 2015, 140 p.
150. **Piret Pikma.** Interfacial structure and adsorption of organic compounds at Cd(0001) and Sb(111) electrodes from ionic liquid and aqueous electrolytes: an *in situ* STM study. Tartu, 2015, 126 p.
151. **Ganesh babu Manoharan.** Combining chemical and genetic approaches for photoluminescence assays of protein kinases. Tartu, 2016, 126 p.
152. **Carolin Siimenson**. Electrochemical characterization of halide ion adsorption from liquid mixtures at Bi(111) and pyrolytic graphite electrode surface. Tartu, 2016, 110 p.
153. **Asko Laaniste.** Comparison and optimisation of novel mass spectrometry ionisation sources. Tartu, 2016, 156 p.
154. **Hanno Evard.** Estimating limit of detection for mass spectrometric analysis methods. Tartu, 2016, 224 p.
155. **Kadri Ligi.** Characterization and application of protein kinase-responsive organic probes with triplet-singlet energy transfer. Tartu, 2016, 122 p.
156. **Margarita Kagan.** Biosensing penicillins' residues in milk flows. Tartu, 2016, 130 p.
157. **Marie Kriisa.** Development of protein kinase-responsive photo-luminescent probes and cellular regulators of protein phosphorylation. Tartu, 2016, 106 p.
158. **Mihkel Vestli.** Ultrasonic spray pyrolysis deposited electrolyte layers for intermediate temperature solid oxide fuel cells. Tartu, 2016, 156 p.

159. **Silver Sepp**. Influence of porosity of the carbide-derived carbon on the properties of the composite electrocatalysts and characteristics of polymer electrolyte fuel cells. Tartu, 2016, 137p.
160. **Kristjan Haav**. Quantitative relative equilibrium constant measurements in supramolecular chemistry. Tartu, 2017, 158 p.
161. **Anu Teearu**. Development of MALDI-FT-ICR-MS methodology for the analysis of resinous materials. Tartu, 2017, 205 p.